Pulmonary Toxicity of Ultrafine Colloidal Silica in Mice

コロイド状シリカ超微細粒子曝露によるマウスにおける肺毒性

Kaewamatawong Theerayuth

Thesis submitted to the United Graduate School of Veterinary Science
at Yamaguchi University in partial fulfillment of the requirements
for the degree of Doctor of Philosophy

Akinori Shimada, Ph.D., Chair
Takehito Morita, Ph.D.
Toshiharu Hayashi, Ph.D.
Susumu Tateyama, Ph.D.
Masato Uehara, Ph.D.

The United Graduate School of Veterinary Science
Yamaguchi University

2006

ABSTRACT

Pulmonary Toxicity of Ultrafine Colloidal Silica in Mice

Kaewamatawong Theerayuth

Ultrafine colloidal silica particles (UFCSs) became widely used in many industries and available for various applications. However, there are limited data of pulmonary toxicity of UFCSs. This research project consisted of two parts. In the first part, we have intratracheally instilled mice to high dose of 3 mg of UFCSs or fine colloidal silica (FCSs) to study pulmonary toxicity of colloidal silica and compare the size effects. The histopathological and electron microscopic results showed that UFCSs induced more severe pulmonary inflammation and tissue damages than FCSs. Larger surface area of UFCSs might be an important factor in the induction of lung tissue injury. In the second part, the purpose of this study was to determine the acute and subacute lung toxicity of low dose of UFCSs in terms of dose and time response. The results from bronchoalveolar lavage, histopathological and immunohistochemical analysis demonstrated that instillation of a low dose of 30 μg of UFCSs can cause transient acute moderate lung inflammation and tissue damage. Oxidative stress and apoptosis may underlie the lung tissue injury induction. The data from the dose and time responses in this study may be useful in predicting the acute and subacute effects of UFCSs on lungs and used as quantitative references to estimate exposure limit for occupational exposure.

TABLE OF CONTENTS

GENERAL INTRODUCTION AND BACKGROUND

Air pollution is a major environmental health problem affecting developed and developing countries around the world especially in megacities. Millions of people living in the largest cities in Asia are being exposed to some of the highest air pollution levels in the world. Levels of air pollution in Asian cities regularly exceed World Health Organization (WHO) recommended guidelines and national air quality standards. In many Asian cities including Bangkok, the air pollution has become a serious cause of lung diseases and breathing disorders. Every year millions of people die or suffer serious health effects from air pollution: mainly respiratory diseases, asthma, chronic obstructive pulmonary disease, cardiovascular disease and cancer of the lung. The most typical urban pollutants include particulate matter (PM), sulphur dioxide (SO_2), volatile organic compounds (VOCs), lead (Pb), carbon monoxide (CO), carbon dioxide (CO_2) and nitrogen oxides (NOx).

- **Particulate matter**

Particulate matter is the general term used for a suspended mixture of solid and liquid particles that are dispersed into ambient air originating from a large variety of anthropogenic and natural sources. The main sources of PM are traffic, energy production using fossil fuels and biomass, industrial source, resuspension of soil, and sea salt spray, but the relative contribution of different sources varies greatly in time and location. These particles can be classified in several ways. Firstly, they can be classified into primary and secondary particles based on the mechanism of their formation. Primary particles are released directly into the atmosphere from sources of generation. Secondly,

particles can be classified by their physical size; the size is from a few nanometers (nm) to tens of micrometers (μm) in diameter. Particle size is the most important determinant of the properties of particles and it has implications on formation, physical and chemical properties, transformation, transport, and removal of particles from the atmosphere. In the measurement of number concentration, particle size segregation is often based on the electrical mobility, whereas in the measurement of mass concentration the segregation is mostly based on aerodynamic diameter. Particle size is normally given as the aerodynamic diameter, which refers to the diameter of a unit density sphere having a terminal velocity equal to that of the given particle. The notation PM_X refers to particulate matter comprising particles less than X μm in diameter. Atmospheric particulate matter is commonly divided into ultrafine ($PM_{0.1}$), fine ($PM_{2.5}$) and coarse particle size ($PM_{2.5-10}$) fractions, which refer to particles with an aerodynamic diameter smaller than 0.1 μm or 2.5 μm or in the range of 2.5-10 μm, respectively. The term total suspended particles (TSP) refer to the aggregate of solid or liquid matter in air. Particles vary in size (up to 45 μm in diameter) and may remain suspended in the air a few seconds to several months.

Most particles larger than 10 μm in aerodynamic diameter are deposited in the nasopharyngeal region and can not penetrate very far into the lungs. Particles between 2.5 and 10 μm are deposited in the nasopharyngeal and the trachea-bronchial parts of the respiratory system and will be caught by cilia lining the wall of the bronchial tubes; the cilia move the particles up and out of the lungs. Particles smaller than 2.5 μm can penetrate deeper into the pulmonary alveoli especially ultrafine size of particles. Since the number-size distribution reaches a maximum in the ultrafine range, this means that the particles getting deposited in the alveoli are small enough to be taken up in the vascular system,

small enough to reach the interstitial spaces of the lung tissue, evade clearance by macrophages and have a small mass median with a relative large surface. The relative large surface of this particle size may carry toxicants into the deep lung and release them quickly (Weijers et al., 2001).

- **Health effects related to particulate matter**

Increased awareness of health problems related to air pollution arising from urbanization and industrialization has, especially during the last two centuries, gradually created a demand for more efficient emission controls, especially in the developed world. Recently, problems caused by atmospheric particulate matter in urban air have received greater attention. Various health effects attributable to PM have been documented (Brunekreef and Holgate 2002; WHO, 2003). Epidemiological studies have consistently associated the current much lower mass concentrations of urban PM_{10} particles with a whole variety of morbidity as well as excess mortality among susceptible population groups such as asthmatic subjects, elderly cardiorespiratory patients and children (Donaldson *et al.*, 2000; Pope III, 2000; USEPA, 2004). The most conclusive evidence has been provided by cohort and time series studies that have linked elevated concentrations of PM_{10} or $PM_{2.5}$ to increased morbidity and mortality (Dye et al., 20001, Pope et al. 2002, Samet et al. 2000). The majority of recent health studies suggest that $PM_{2.5}$ arising mainly from man-made sources are more harmful than PM_{10} (WHO, 2003; USEPA, 2004).

Ultrafine particles have been suggested to pose a great risk to human health due to their high number concentration in urban environments and ability to penetrate from the lung alveoli into the blood circulation (Delfino et al. 2005; Nemmar et al. 2002). In addition,

because of the high specific surface area, ultrafine particles are attributed to have specific toxicity, which might result in the induction of oxygen radicals and in the catalysis of chemical reactions (Donaldson et al. 2001; Kreyling et al, 2006). The dosimetry, deposition patterns in the different regions of the respiratory tract and the biokinetic fate of ultrafine particles in the body is not fully understood. Ultrafine particles are found to a large extent in urban environmental particulate air pollution and are the predominant particle size by number in urban PM_{10}. Ultrafine particles also have important industrial applications-for example, as ultrafine carbon black and titanium dioxide-and so there is potential for occupational exposure. However, the extent of the risk to workers has not yet been assessed (Donaldson et al. 2001).

- **Evaluation of health effects of particulate matter**

The health effects of particulate matter have been explored in both epidemiological and toxicological studies. *Epidemiology* is the science that studies the factors that determine or influence the incidence or distribution of disease and other health-related events and their causes in a defined human population (Merriam Webster's 2002). *Toxicology* is the science that studies poisons, their actions, their detection and the treatment of the conditions produced by them (Merriam Webster's 2002). The purpose of toxicological studies is to produce supportive evidence for the epidemiological findings on the organ-specific mechanisms of action (biological plausibility), as well as provide additional information on the responsible sources and physicochemical characteristics of the particulate matter causing the effects. Toxicological studies can be made by exposing human or animal lungs or cultured target cells (e.g. macrophages, respiratory epithelial

cells) to particulate matter either by inhalation, or by instillation in an aqueous medium. In inhalation exposure, there is no advance control over the condition or dose to which the humans, animals or cultured cells are exposed. Advance particle collection and the instillation method is therefore the only realistic way of investigating the relationship of the dose and chemical composition of size-segregated particulate matter to toxic activities (e.g. inflammation, cytotoxicity, genotoxicity). Both instillation and inhalation methods have given virtually similar results on particulate-induced inflammatory toxicity (Costa *et al.*, 2006). The instillation method allows advance selection of the particulate samples and mass doses to be used in the study. A comparison of the toxic activities of particulate samples in different pollution situations is typically made on an equal mass basis for each size range, which emphasizes the importance of knowing the exact dose to which the human or animal airways.

- **Air pollution and particulate matter problem in Bangkok**

High levels of urbanisation have resulted in increasing urban air pollution due to transportation, energy production and industrial activity all concentrated in densely populated urban areas. Bangkok serves as the capital and the economic center of Thailand, with the largest population density of any city in Thailand. In many Asian cities including Bangkok, the air pollution is increasingly posing a significant threat to the health, quality of life and environment of the urban population. It is usually to see Bangkok residents on the street covering their noses and mouths with surgical masks to protect themselves from the hazardous fumes. The major sources of air pollution in Bangkok come from vehicle exhaust, industrial and building demolition. In addition, the burning of biomass such as firewood,

agricultural and animal waste in some cities around Bangkok contributes to the level of pollution. In Bangkok the level of airborne particulate matter is monitored by The Pollution Control Department (PCD), Ministry of Natural Resources and Environment. PCD reports 6 air pollutant parameters daily including sulfur dioxide (SO_2), nitrogen dioxide (NO_2), carbon monoxide (CO (1 hr), CO (8hr)), ozone and particular Matter (PM_{10}). According to the summary report of state of Thailand's pollution in Year 2005, the major air pollutant continues to be particular matter. The maximum PM_{10} concentration along the roadside average exceeded the standard every year (Figure 1). Monitoring results indicate that Bangkok has a serious air pollution situation.

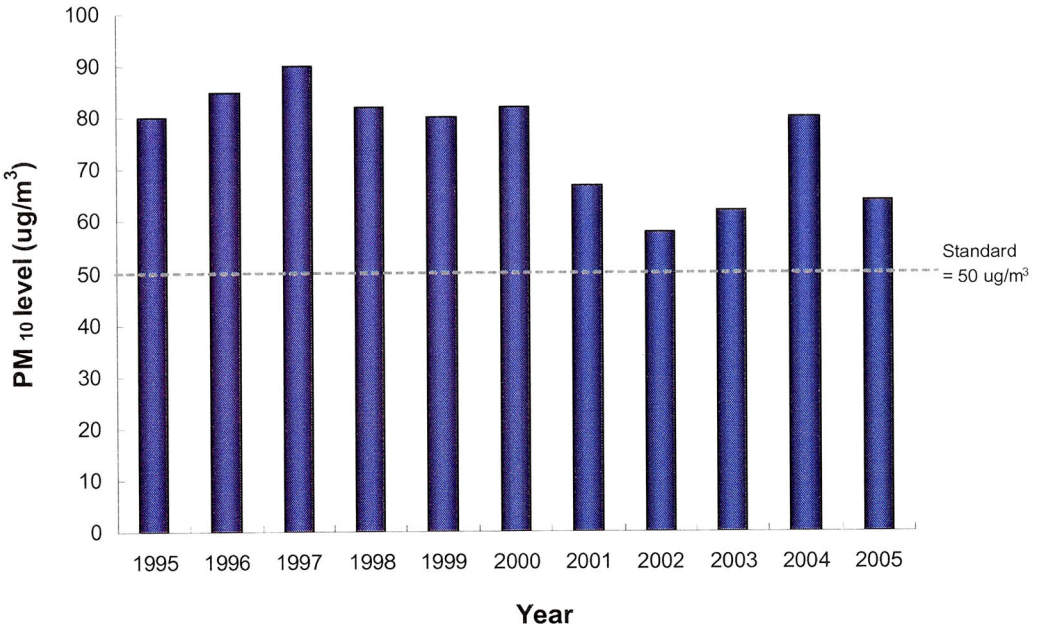

Figure 1. Level of PM_{10} (1-year average) from road-side stations in Bangkok during 1995-2005

Source: Pollution Control Department, Ministry of Natural Resources and Environment.

Epidemiological studies indicate that exposure to particulate matter can lead to adverse effects on human health. Although a clear causality has not yet been established, it is widely suspected that elevated concentrations of PM_{10} in Bangkok are responsible for negative health outcomes. Every year a lot of people die or suffer serious health effects from air pollution: mainly respiratory diseases, asthma, chronic obstructive pulmonary disease, cardiovascular disease and cancer of the lung. Chulalongkorn University, Thailand, had studied to evaluate the effects of particulate matters towards student's health and found that students in the areas of high airborne dust concentrations (PM_{10} >100 mg/m^3) had a higher prevalence of respiratory disease than students living in the areas of low dust concentration (PM_{10} <50 mg/m^3). Moreover, the daily variation of respiratory symptoms was associated with fluctuation of PM_{10} levels (Public Health College, 1995). It was also found that the inpatient rate of cardiovascular and respiratory diseases had increased while the PM_{10} levels increased. In the area without air-conditioning, dust level was rather high (180 mg/m^3). The adult who lived in the area of high dust had about twice time risk in developing acute respiratory disease compared to those living in a clean air atmosphere. It was anticipated that, with the current PM_{10} level, there would be 4,000 to 5,500 premature deaths each year due to airborne dust exposure estimated from 10 million populations (Hagler Bailly Services, Inc, 1998). High levels of urban air pollution also have economic implications due to increased mortality and illness, damage to crops and property and loss of tourism. The World Bank (1996) estimated that a 20 percent reduction of key pollutants in Bangkok would provide health benefits of approximately US $4 million to $1.6 billion for PM. Traffic congestion is a major problem in Bangkok and the World Bank estimated that a 10 per cent reduction in peak-hour trips would provide benefits of approximately US

$400 million annually.

- **Definition and health effects of silica**

Silica is a group of naturally occurring minerals that exist both in a variety of crystalline and amorphous forms, which comprise silicon and oxygen (SiO_2) with trace amount of Al, Fe, Mn, Mg, Ca and Na in their structure. The principal naturally occurring crystalline silica exists as quartz; three other forms of crystalline silica are cristobalite, tridymite, and tripoli. Although identical chemically (SiO_2 form), they differ from each other in their crystal parameters. The basic structural units of the silica minerals are silicon tetrahedra arranged such that each oxygen atom is common to two tetrahedra. However, there are considerable differences in the arrangements of the silicon tetrahedra among the various crystalline forms of silica (Coyle, 1982). Crystalline silica is widely used in industry and has long been recognized as a major occupational hazard, causing disability and deaths among workers in several industries. Occupational exposure to crystalline silica dust is associated with an increased risk for pulmonary diseases such as silicosis, pulmonary tuberculosis, chronic bronchitis, chronic obstructive pulmonary disease (COPD), extrapulmonary disease and lung cancer (Merget et al., 2002). The most frequently occurring pathologic effects of silica are multiple nodular lesions in lung parenchyma, bronchial associated lymphoid tissue, lymph nodes, and other viscera and fibrotic lesions of the pleura. Nodular lesions in the lungs may develop by conglomeration into large lesions of progressive massive fibrosis (American Thoracic Society, 1997).

Amorphous silica also is composed of SiO_2, but the SiO_2 molecule is randomly linked, forming no repeating pattern. Naturally occurring sediments or rock that contain

amorphous forms of silica include diatomite or diatomaceous earth, a hydrated form (e.g., opal), and an unhydrated form (e.g., flint). Commonly encountered synthetic amorphous silicas, according to their method of preparation, are silica gel, precipitated silica, fumed silica and colloidal silica. The most outstanding characteristics of synthetic amorphous silicas are their small ultimate particle size and high specific surface area, which determine their numerous applications. According to the different physicochemical properties, the major classes of synthetic amorphous silica are used in a variety of products, e.g. as fillers in the rubber industry, in tyre compounds, as free-flow and anti-caking agents in powder materials, and as liquid carriers, particularly in the manufacture of animal feed and agrochemicals; other uses are found in toothpaste additives, paints, silicon rubber, insulation material, liquid systems in coatings, adhesives, printing inks, plastisol car undercoats, and cosmetics. Animal inhalation studies with intentionally manufactured synthetic amorphous silica showed at least partially reversible inflammation, granuloma formation and emphysema, but no progressive fibrosis of the lungs. Epidemiological studies do not support the hypothesis that amorphous silicas have any relevant potential to induce fibrosis in workers with high occupational exposure to these substances (Merget et al., 2002).

Ambient crystalline silica is emitted into the environment as a fractional component of PM_{10}. Environmental emissions of silica can arise from natural, industrial, and farming activities. Recently, public concern regarding nonoccupational or ambient silica exposure, mainly to crystalline silica, has emerged making it important to evaluate background and ambient concentrations. The relationship between PM_{10} and its crystalline silica component will vary depending on regional environmental and source characteristics. However, no

data on ambient air concentrations of amorphous silicas were located. Ambient emissions of silica rarely are estimated or measured in air pollution studies of particulate matter. In general, it is more likely that occupational crystalline silica exposures have been studied. The data available on nonoccupational exposures to other forms of silica are extremely limited (USEPA, 1996).

Colloidal silica consists of stable dispersion amorphous silica particles. To achieve this, the silica particles must be small enough such that they are largely unaffected by gravity. Therefore, silica particle sizes are usually of the order of less than 100 nanometers (ultrafine size). The term colloid refers to the suspension, where the sols are the tiny discrete particles in suspension. Colloidal silica can be manufactured from materials such as sodium silicate and are usually available in varying concentrations to suit various applications. Colloidal silica is available for various applications such as fiber, sizing, diazo paper's manufactures, cellophane film, precision casting, ceramics, glass fiber, paints, catalysts, batteries, wax, optics, elastomer, food, health care, industrial chromatography and polishing. Nanoengineered colloidal silica particles are currently interest for slurries used by semiconductor manufacturers for electronic precision polishing or planarisation applications such as chemical mechanical planarisation and silicon wafer polishing. The market for this material is estimated to grow rapidly world wide. However, the data of the adverse effects of nanoengineered colloidal silica in the biological species, human health and environment have been limited and not clearly assessed.

OBJECTIVE OF THE STUDY

The overall objective of this thesis was to add to current knowledge on acute and subacute toxicological studies of colloidal silica in mice using biological and pathological evaluations.

In chapter 1, the specific aims of the study were

- to describe acute pulmonary pathological effects caused by intratracheal exposure to colloidal silica.
- to compare the size effects between ultrafine (UFCSs) and fine (FCSs) colloidal silica particles.

In chapter 2, the specific objectives were

- to determine the biological and pathological effects of intratracheally instilled low dose of UFCSs on the lungs of mice in terms of dose and time response during the acute and subacute stages.
- to investigated some factors that could be important in the induction of pulmonary toxicity of UFCSs.

LIST OF ORIGINAL PUBLICATIONS

This thesis is based on the following original publications.

- Kaewamatawong, T., Kawamura, N., Okajima, M., Sawada, M., Morita, T., and Shimada, A. (2005). Acute pulmonary toxicity caused by exposure to colloidal silica: particle size dependent pathological changes in mice. *Tox. Pathol.* **33,** 745-751.
- Kaewamatawong, T., Shimada, A., Okajima, M., Inoue, H., Morita, T., Inoue, K., and Takano, T. (2006). Acute and subacute pulmonary toxicity of low dose of ultrafine colloidal silica particles in mice after intratracheal instillation. *Tox. Pathol.* **34,** 958-965.

CHAPTER 1

Acute Pulmonary Toxicity Caused by Exposure to Colloidal Silica

: Particle Size Dependent Pathological Changes in Mice

Abstract

To compare the pulmonary toxicity between ultrafine colloidal silica particles (UFCSs) and fine colloidal silica particles (FCSs), mice were intratracheally instilled with 3 mg of 14-nm UFCSs and 230-nm FCSs and pathologically examined from 30 min to 24 hr post-exposure. Histopathologically, lungs exposed to both sizes of particles showed bronchiolar degeneration and necrosis, neutrophilic inflammation in alveoli with alveolar type II cell proliferation and particle-laden alveolar macrophage accumulation. UFCSs, however, induced extensive alveolar hemorrhage compared to FCSs from 30 min onwards. UFCSs also caused more severe bronchiolar epithelial cell necrosis and neutrophil influx in alveoli than FCSs at 12 and 24 hr post-exposure. Laminin positive immunolabellings in basement membranes of bronchioles and alveoli of UFCSs treated animals was weaker than those of FCSs treated animals in all observation times. Electron microscopy demonstrated UFCSs and FCSs on bronchiolar and alveolar wall surface as well as in the cytoplasm of alveolar epithelial cells, alveolar macrophages and neutrophils. Type I alveolar epithelial cell erosion with basement membrane damage in UFCSs treated animals was more severe than those in FCSs treated animals. At 12 and 24 hr post-exposure, bronchiolar epithelial cells in UFCSs treated animals showed more intense vacuolation and necrosis compared to FCSs treated animals. These findings suggest that UFCSs has greater ability to induce lung inflammation and tissue damages than FCSs.

Keywords: acute pulmonary toxicity, colloidal silica, electron microscopy, fine, intratracheal instillation, mice, ultrafine.

Introduction

Amorphous silica is a naturally occurring or synthetically produced oxide of silicon characterized by the absence of pronounced crystalline structure, and which has no sharp peaks in its X-ray diffraction pattern (Van Niekerk et al., 2002). There are several types of amorphous silica including fumed silica, colloidal silica, diatomaceous earth and precipitated silica. A number of studies have reviewed the adverse effects of amorphous silica; this silica has potential to induce transient pulmonary inflammation but changes may regress during the recovery period compared to persistent pulmonary inflammation by crystalline silica (Pratt, 1983; Reuzel et al., 1991; Warheit et al., 1995). In humans, an epidemiologic investigation in occupational exposure to amorphous silica generally showed no evidence of silicotic effect and any potential for carcinogenicity (McLaughlin et al., 1997). However, in an occupational setting study, a significant decrease in lung function was observed after amorphous silica exposure (Choudat et al., 1990).

Colloidal silica is one of synthetically amorphous silica that consists of stable dispersion spherical silica particles. The particle sizes are usually of the order from 10 micrometers to less than 10 nanometers. Recently, the colloidal silica became widely used in many industries and available for various applications. Toxicological characteristics of the colloidal silica are characterized fairly well as being less toxic than crystalline forms in experimental animals. Kelly and Lee (1990) reported that inhalation of 50 or 150 mg/m^3 Ludox colloidal silica for 4 weeks produced dose-related pulmonary effects characterized by accumulation of silica-dust-laden alveolar macrophages, neutrophilic infiltration, and Type II epithelial cell hyperplasia. The severity and incidence of pulmonary lesions were

reduced after a 3-month recovery period, most particle-laden alveolar macrophages (AMs) had disappeared and the remaining AMs were aggregated and sharply demarcated, although small number of silicotic lesions were described and lymph nodes were enlarged. They concluded the no-observable-effect level (NOEL) was 10 mg/m^3. Traditional inhalation toxicity study clearly demonstrated that Ludox colloidal silica is far less active in producing pulmonary effects when compared to Minusil crystalline silica (Warheit et al, 1995). Moreover most of the biochemical parameters such as lactate dehydrogenase, total protein and N-acetyl glucosaminidase (NAG) returned to control values after a 3- month recovery period. In a subchronic inhalation study of Ludox colloidal silica, Lee and Kelly (1993) demonstrated the evidence of the transmigration of particle-laden alveolar macrophage from the alveoli to the interstitium and the tracheo-bronchial lymph node (TBLN) via interstitial lymphatics. In addition, subsequent intra-alveolar silicotic granuloma formations in the interstitium were also observed in the study.

Ultrafine particles (UFP) are commonly defined as particles with diameter less than 100 nm that are ubiquitous in urban ambient air as both singlet and aggregated particles. Ultrafine particulates represent a substantial component in terms of particle numbers in PM_{10} (particulate matter < 10 μm aerodynamic diameter), although they represent a relatively small fraction of the total mass. Currently, the potentially harmful role of ultrafine particle, receives considerable attention as a possible explanation for the epidemiological associations of increase in PM_{10} with health effects (Donaldson et al., 2001). Many toxicological studies makes it clear that ultrafine particles of various types can cause lung inflammatory responses, epithelial cell hyperplasia, inhibit phagocytosis, increased chemokine expression, lung fibrosis, increased oxidant-generating abilities, and

lung tumors (Zhang et al., 1998a and 1998b; Brown et al., 2000; Donaldson and MacNee, 2001; Warheit, 2004). Ultrafine particles are also implicated as of the adverse effects of particulate air pollution on the cardiovascular system by the induction of airway inflammation, leukocyte expression, increased endothelial adhesion molecule in blood, change in blood coagulability and alteration of cardiac electrical activity (Frampton, 2001; Nemmar et al., 2002; Donaldson and Stone, 2003; Gilmour et al., 2004). It has been demonstrated that ultrafine particles cause greater inflammatory responses and the development of particle-mediated lung diseases than the fine particles per given mass (Li et al., 1999; Nemmar et al., 2003).

Data of the pulmonary pathological effects of amorphous colloidal silica in experimental animals are limited and precise mechanisms of the induced pathological changes are not clearly understood. To date, there is no pathological report on comparative pulmonary toxicity of fine and ultrafine colloidal silica. The purpose of this study is to describe acute pulmonary pathological effects caused by intratracheal exposure to amorphous colloidal silica and compare the size effects in light and electron microscopy.

Materials and Methods

Experimental animal

Female ICR mice, weighing 28-34 g and at 10-12 weeks of age were purchased from CLEA Japan, INC. The mice were housed in an animal facility under 12/12 hr light/dark cycle, temperature of 24 ± 1 °C, relative humidity of 55 ± 10% and negative atmospheric pressure. They were provided with mouse chow and filtered tap water *ad libitum* throughout the experiment. All animal experiments were performed according to the National Institute for Environmental Studies guidelines for animal welfare.

Particles

Ultrafine colloidal silica (Grade PL-1) was obtained as a gift from Fuso Chemical Co.,Ltd., Japan. and had a primary particle diameter of 14 nm (Lot No. R2Z007). The silica particles were suspended in water at a concentration of 120 mg/ml.

Fine colloidal silica (Grade PL-20) was also supplied by the same company and had a primary particle size of 213 nm (Lot No. Y1Y001). The particles were suspended in water at a concentration of 239 mg/ml.

Experimental design

45 mice were randomly divided into five control and ten exposure groups of 3 animals each. Ten exposure groups were exposed to 50 µl aqueous suspensions of 3 mg of ultrafine and fine colloidal silica in Milli-Q® purified water by intratracheal instillation. The control groups of mice were instilled to 50µl of Milli-Q® purified water. Animals in each group were sacrificed at 30 min, 2, 6, 12 and 24 hr after instillation.

Histopathology

After gross examination of respiratory organs such as lungs and hilar lymph nodes, the lungs and trachea were removed *en bloc* and instilled with 10% buffered neutral formalin. Whole lungs and hilar lymph nodes were processed according to routine histological techniques. After paraffin embedding, 3 µm sections were cut and stained with hematoxylin and eosin (H&E) for histopathologic evaluation.

Laminin immunohistochemistry

Tissue sections from lung were immunostained by using avidin-biotin complex (ABC) method, in which labeled Streptavidin biotin (LSAB) kit (DAKO, Glostrup, Denmark) was included. After deparaffinization of the sections, the sections were treated with proteinase K for 30 min at 39 °C. The sections were incubated with 3% H_2O_2 to quench endogenous peroxidase for 15 min at room temperature and then with 10% normal goat serum for 5 min in microwave oven 250 w to inhibit nonspecific reactions. Thereafter the sections were reacted over night at 4 °C with Rabbit anti-laminin monoclonal antibody diluted 1:200 (SIGMA®, DAKO, Glostrup, Denmark). The peroxidase conjugated goat anti-rabbit IgG diluted 1:400 (DAKO, Glostrup, Denmark) was reacted to sections as a secondary antibody in microwave oven 200 w for 7 min. The positive reactions resulted in brown staining with the substrate 3,3'-diaminobenzidine tetrahydrochloride (DAB), and the sections were counterstained with hematoxylin.

Electron microscopy

For transmission electron microscopy, lung tissue samples fixed with 10% buffered neutral formalin were rinsed in 0.1 M phosphate buffer (pH = 7.4), post-fixed in 1% osmium tetroxide, dehydrated with serial alcohol and embedded in epoxy resin. Semithin

(1-μm thick) sections were stained with toluidine blue to select and locate areas of interest for electron microscopic examination. Ultrathin sections stained with uranyl acetate and lead citrate were examined with a JEM-100CX electron microscope (JEOL, Tokyo, Japan).

Results

Characteristics of fine and ultrafine colloidal silica

The scanning electron microscopic images of ultrafine (UFCSs) and fine (FCSs) colloidal silica are shown in figure 1A and 1B. Both sizes of colloidal silica particles had a compact and spherical configuration. There was substantial difference in diameter between UFCSs (average size of 14 nm) and FCSs (average size of 213 nm). The surface area, which measured by Brunauer, Emmett and Teller (BET) method, was also much greater for UFCSs than FCSs particles, 194 and 13 m^2/g, respectively. There was also a difference between UFCSs and FCSs in terms of metal composition, but both had very low levels (potassium, aluminium, magnesium < 0.01 ppm; Iron < 0.005 ppm ; data were supplied by Fuso Chemical Co., Ltd., Japan). However, FCSs had a little more of sodium (0.10 ppm) and calcium (0.02 ppm) than UFCSs (sodium = 0.05 ppm and calcium < 0.01 ppm).

Clinical and gross findings

In FCSs treated animals, there were no exposure–related clinical signs in any observation time. Some mice in UFCSs treated animals showed a sign of dyspnea and died shortly after instillation (data are not shown). Grossly, instillation of UFCSs and FCSs caused congestion, edema and hemorrhage in lung compared to the control groups. The degree of lung hemorrhage in UFCSs was more severe than FCSs treated animals at all observation times (Figure 2). In both UFCSs and FCSs treated animals, tiny pin-head sized white foci were scattered particularly in the pleural surface of lung lobes. At all time points, the hilar lymph nodes from UFCSs and FCSs treated animals were slightly enlarged compared to the control animals.

Light microscopy

Lungs from control animals instilled with Milli-Q® purified water showed normal bronchiolar and alveolar architectures with occasional mild congestion in the alveoli (Figure 3A). Treated animals showed hemorrhage, neutrophilic inflammation, degeneration and necrosis of lining epithelial cells throughout the airway from the large bronchioles to terminal bronchioles and alveoli. By 30 min after instillation of UFCSs and FCSs, the lungs showed degeneration, attenuation and desquamation of some bronchiolar epithelial cells; increased numbers of neutrophils and alveolar macrophages were also observed in alveoli with some swollen alveolar type II epithelial cells. However, more intense alveolar hemorrhage was observed in the UFCSs treated animals compared to FCSs treated animals (Figure 3B, 3C). The hilar lymph nodes of both UFCSs and FCSs treated animals were slightly enlarged with neutrophil infiltration in subcapsular and medullary sinus. At 2 and 6 hr after instillation, the lesions in the lungs and hilar lymph nodes of both UFCSs and FCSs treated animals were similar to those seen in 30 min post-exposure, but the lung lesions of UFCSs treated animals were more severe than FCSs treated animals. Attenuation of bronchiolar epithelial cells and accumulation of particle-laden alveolar macrophages (AMs) were observed (Figure 3D, 3E). Lungs of mice killed at 6 hr after UFCSs instillation showed more severe bronchiolar epithelial cell desquamation than those of FCSs treated animals. By 12 hours after instillation, UFCSs caused marked degeneration, attenuation and necrosis of bronchiolar epithelial cells, whereas FCSs caused mild degenerative effects (Figure 3F, 3G); both UFCSs and FCSs treated animals showed a significant influx of neutrophils scattering around the alveoli that contained particles. At 24 hr post-exposure, UFCSs induced more extensive inflammatory changes than FCSs; marked increase of

neutrophils sharply demarcated from the remaining normal alveoli were associated with these changes (Figure 3H, 3I). A number of nodular aggregate of neutrophils and particle-laden AMs were observed in some alveolar regions particularly in perivascular areas adjacent to the bronchioles. The nodular lesions consisted of clumps of free particles, some cell debris and particle-laden AMs, and neutrophils. Severe degeneration and necrosis of bronchiolar epithelial cells were still observed in the UFCSs treated animals.

Laminin immunohistochemistry

In control lung tissues, laminin stainings were expressed as a thin and continuous line in bronchial basement membrane, blood vessel basement membrane, around bronchial gland and along alveolar septa (Figure 4A). Weak and scarcely positive staining was observed in discontinuous pattern along basement membranes of bronchioles and alveoli of mice exposed to UFCSs and FCSs. The basement membranes of the alveoli containing clumps of particles and inflammatory cells showed interruptions with a patchy distribution of the immunoreactivity (Figure 4B, 4C). The positive reaction was weaker in the UFCSs treated animals compared to FCSs treated animals in all observation times especially at 24 hr post-exposure.

Electron microscopy

Morphology and distribution of particles in lungs

Two forms of UFCSs, singlet and aggregate forms, were observed in lung tissues. Almost all of singlet UFCSs were spherical, compact electron-dense particles with diameters approximately 10-14 nm. On the other hand, aggregates (diameter > 100 nm) of UFCSs were dominant which consisted of chains and clusters of UFCSs (Figure 5A). The ultrastructural findings of FCSs also appeared as compact, spherical electron-dense

particles with diameter approximately 213 nm, but all of FCSs remained separated and showed rarely the agglomerated pattern (Figure 5B).

Numerous free particles were observed on the bronchiolar epithelial cell surface and along the apical surface of the plasma membrane of alveoli in both UFCSs and FCSs treated animals even at 24 hr post-exposure. Accumulation of particle-laden AMs was also found in the alveoli and bronchiolar lumens. These particle-laden AMs showed round or polygonal shapes with numerous lysosomes and phagolysosomes containing particles (Figure 5C, 5D). Instilled particles were also observed in the cytoplasm of neutrophils that were presented around clumps of particles (Figure 5E, 5F). Many singlet FCSs were seen in type II alveolar epithelial cell cytoplasm, in which some particles were occasionally observed in lamellar bodies (Figure 5G, 5H). There were a few particles in the cytoplasm of type I alveolar epithelial cells. On the contrary, both singlet and small agglomerated UFCSs were incorporated by both types of alveolar epithelium.

Bronchiolar lesions

Ultrastructural analysis of lungs from UFCSs treated animals revealed significant destructive changes of bronchiolar epithelial cells. Damage to bronchiolar epithelial cells was first observed at 30 min after instillation. The most severe changes, which occurred from 12 to 24 hr after treatment, included swelling of endoplasmic reticulum, necrosis, and sloughing (Figure 6A, 6B). Vacuolation and attenuation of bronchiolar epithelial cells were also observed while the remaining Clara cells showed many mitochondria, irregular arrangement of smooth endoplasmic reticulum (sER) and remarkable edema in the cytoplasm with a few secretory granules (Figure 6C, 6D). Damage and dissociation of basement membranes of some bronchioles were also observed. By contrast, bronchiolar

epithelial cell lesions in FCSs treated animals were similar but less pronounced as compared to the alterations observed in UFCSs treated animals.

Alveolar lesions

The ultrastructure of the lungs from UFCSs treated animals demonstrated marked pathological changes compared to FCSs treated animals. Type I alveolar epithelial cells had features of considerable damage particularly in the areas apposing to the clump of UFCSs particles. There was evidence of advanced injury to type I alveolar epithelial cells, with necrosis and desquamation leading to direct exposure of interstitial tissue to the alveolar space. Damage and dissociation of basement membranes were also found associated with type I alveolar epithelial cell erosion (Figure 6E). The capillary endothelium of the alveolar septa showed features of focal damage with increased numbers of vesicles in their cytoplasm. The vascular lumen displayed numerous neutrophilic granulocytes, which infiltrated through the capillary wall to the area with particle accumulation. The areas of lung parenchyma with neutrophil and alveolar macrophage accumulation showed remarkable damage of the alveolar wall structures.

Discussion

Occupational exposure to crystalline silica dust is associated with an increased risk for pulmonary diseases such as silicosis. Numerous studies on the crystalline silica toxicity in experimental animals showed inflammatory effects and following pulmonary fibrosis and pulmonary dysfunction (Lugano et al., 1982; Reiser et al., 1982; Callis et al., 1985). While the pulmonary toxicity of crystalline silica is widely known, there is limited information regarding the lung toxicity by amorphous silica. Animal inhalation studies with synthetic amorphous silica showed reversible inflammation, granuloma formation and emphysema (McLaughlin, et al., 1997; Merget et al., 2002). Occupational exposure to amorphous silica showed no any relevant potential to induce silicosis. Colloidal silica, one of synthetically made amorphous silica that became widely used in many industries and available for various applications, are known to be far less active in producing pulmonary damage when compared to crystalline silica (Warheit et al., 1991). Subchronic inhalation toxicity studies on colloidal silica reported that inhalation of Ludox colloidal silica produced dose-related pulmonary effects characterized by accumulations of dust-laden polymorphonuclear cells in alveolar ducts, concomitant with neutrophil infiltration and type II alveolar epithelial cell hyperplasia with small numbers of silicotic lesions. The severity and incidence of pulmonary lesions were reduced after a 3-month recovery period (Lee and Kelly, 1992). There are, however, limited data of the acute pulmonary effects after exposure to colloidal silica by intratracheal instillation. To understand acute inflammatory events in the lung following colloidal silica exposure, we exposed mice to UFCSs and

FCSs and examined pulmonary changes by histology, immunohistochemistry and electron microscopy at intervals from 30 min to 24 hr post-exposure.

At 30 min and 2 hr post-exposure, there was the evidence of severe degeneration and necrosis of bronchiolar epithelial cells with clumps of colloidal silica particles on epithelial cell surface, but no evidence of inflammatory reactions around the affected bronchioles. This suggested that colloidal silica has a direct toxic effect on lung epithelial cells and bronchiolar epithelial cells seem to be the first target for colloidal silica toxicity. It is generally accepted that the biological responses to amorphous silica are related to its surface properties. The composition and structure of particle surface functionalities such as hydrophilicity, impurities and specific surface functional group play an important role in the biological responses to silica. Silicon functionalities as well as traces of iron impurities on the silica surface are implicated in free radical release at the surface and in subsurface layers of particles (Vallyathan et al., 1988;Fubini et al., 1990). The specific surface silanol groups (SiOH) of silica are directly involved in both hemolysis (Pandurangi et al., 1990; Hemenway et al., 1993) and toxicity to alveolar cells *in vitro* (Mao et al., 1995; Fubini et al., 1999). It appears that the silanol presence is a prerequisite for the attachment of silica particles to the cell membrane and consequent cellular uptake by macrophages and neutrophils. This hypothesis is supported by the study showing that the silanol groups form hydrogen bonds with some sites on the cell membrane (Shi et al., 1989). Such hydrogen bonding could facilitate the process of phagocytosis. Furthermore, a specific binding of silanol group to the phosphate groups of DNA was reported (Mao et al., 1994). This close proximity between DNA and the active sites of the silica surface would enable the short-lived radicals to induce DNA damage (Saffiotti et al., 1994).

Numerous experimental studies have shown that ultrafine particles have more ability to enhance lung injury than fine particles of the same chemical composition; the studies included a number of diverse materials such as cobalt, nickel, carbon black and TiO_2 (Baggs et al., 1997; Brown et al., 2000; Zhang et al., 2000; Zhang et al., 2003). To our knowledge, there is no detailed pathological report on the pulmonary toxicity induced by different particle sizes of colloidal silica. In the present study, we compared acute pathological findings of lung between UFCSs and FCSs treated animals. The results showed that instillation of UFCSs induced more severe bronchiolar epithelial cell necrosis and purulent inflammation in alveoli than FCSs at 12 and 24 hr post-exposure. Destruction of bronchiolar and alveolar basement membranes was detected as weak positivity of laminin immunolabellings; the immunopositivity in UFCSs treated animals was weaker than those in the FCSs treated animals. These basement membrane damages were associated with particle accumulation. Concomitant ultrastructural studies confirmed more severe damage including dissociation of basement membranes and erosion of type I alveolar epithelial cell in UFCSs treated animals than FCSs treated animals.

Ultrafine particles have a much greater surface area than fine colloidal silica. Several plausible mechanisms have been proposed for the pathogenesis of the initial pulmonary injury following ultrafine particle exposure. The higher toxicity of ultrafine particles than fine particles may be related to the larger surface area per given mass. Higher surface area of particles can play a role as a carrier for co-pollutants such as gases and chemicals, specifically transition metals that could form a coat on the particle surfaces during their formation (Donaldson et al., 2001). Larger surface areas have also been associated with higher inflammatory responses, probably related to increased reactive

oxygen species generation, independent of transition metal exposure. However, results of experimental studies with ultrafine particles composed of low-toxicity materials such as polystyrene have shown an increased inflammatory response with increased total surface area, without any contribution from other factors such as co-pollutants or transition metals. This suggests that surface area drives inflammation in short term and that ultrafine particles induce a greater changes because of the greater surface area they possess (Brown et al., 2001). In addition, it has also been suggested that high numbers of ultrafine particles in the alveolar region may overwhelm the capacity of alveolar macrophages to phagocytoze and allow interaction of particles with epithelial cells, resulting in decreased clearing efficiency of ultrafine particles from the alveoli and leading to epithelial cell injury (Renwick, et al., 2001).

In summary, this study showed detailed pathology of severe acute pulmonary inflammation and tissue injury induced by intratracheal instillation of colloidal silica; ultrafine colloidal silica particles induced more severe changes than fine colloidal silica particles. Larger surface area of particles might be an important factor in the induction of lung tissue injury.

Figures and figure legends

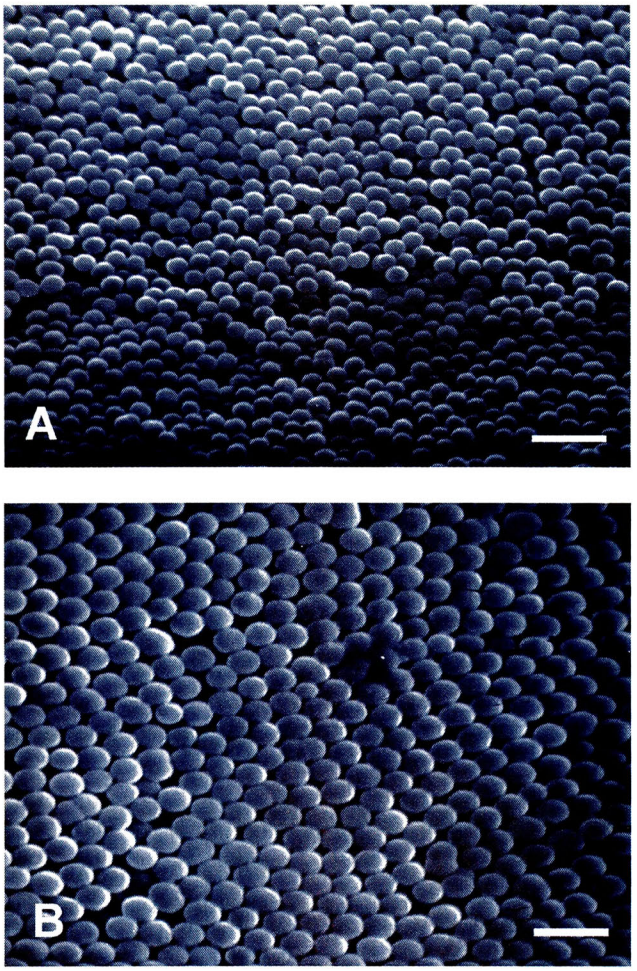

Figure 1. Scanning electron microscopy of ultrafine (A: bar = 50 nm) and fine (B: bar = 480 nm) colloidal silica particles.

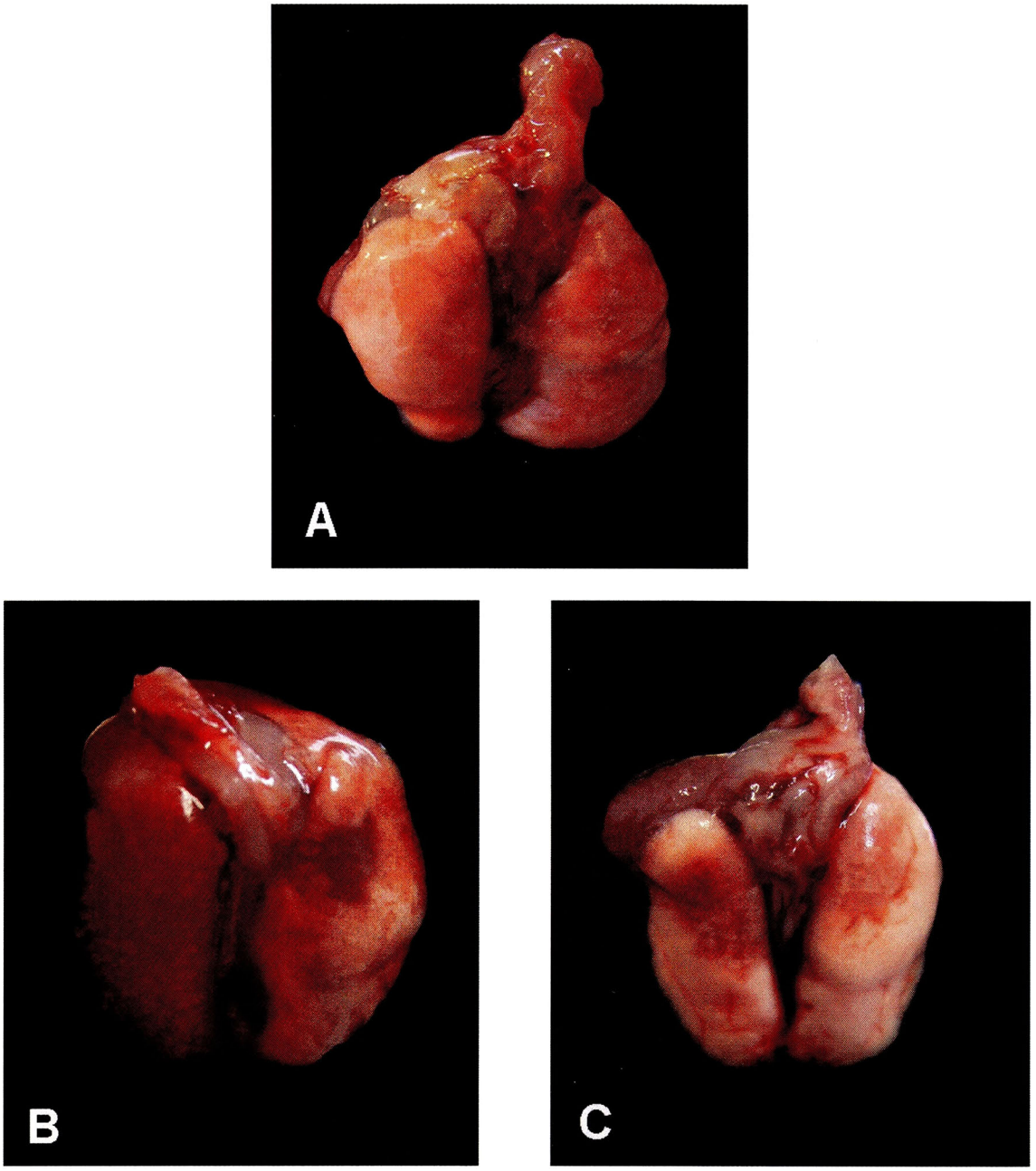

Figure 2. Gross appearances of lungs from control (A), UFCS (B) and FCS (C) treated groups. No significant changes were observed in the control animal. In UFCS treated mouse, the lung shows more severe hemorrhage and edema than FCS treated animal.

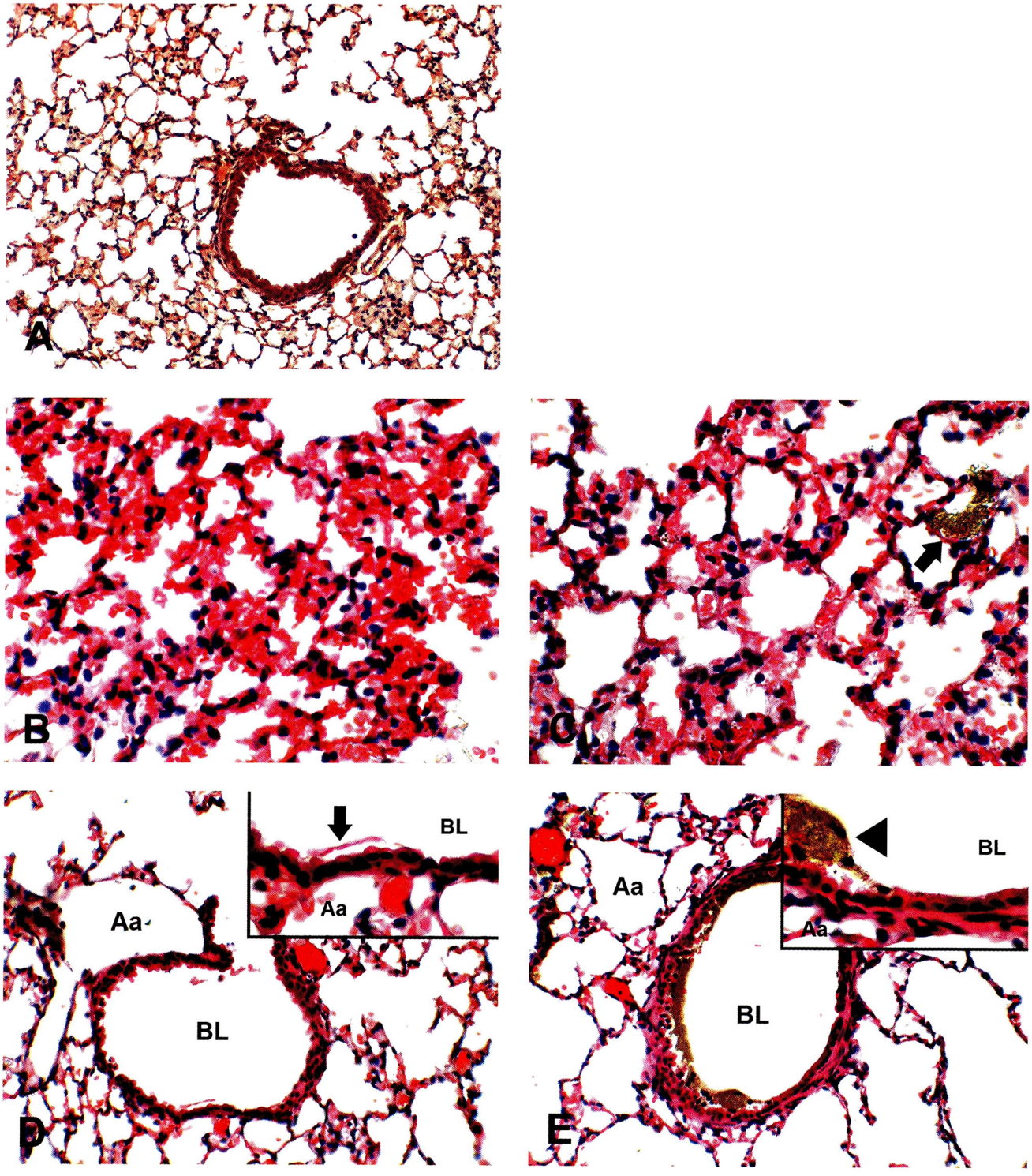
A
B
C
BL
Aa
D
BL
Aa
Aa
BL
E

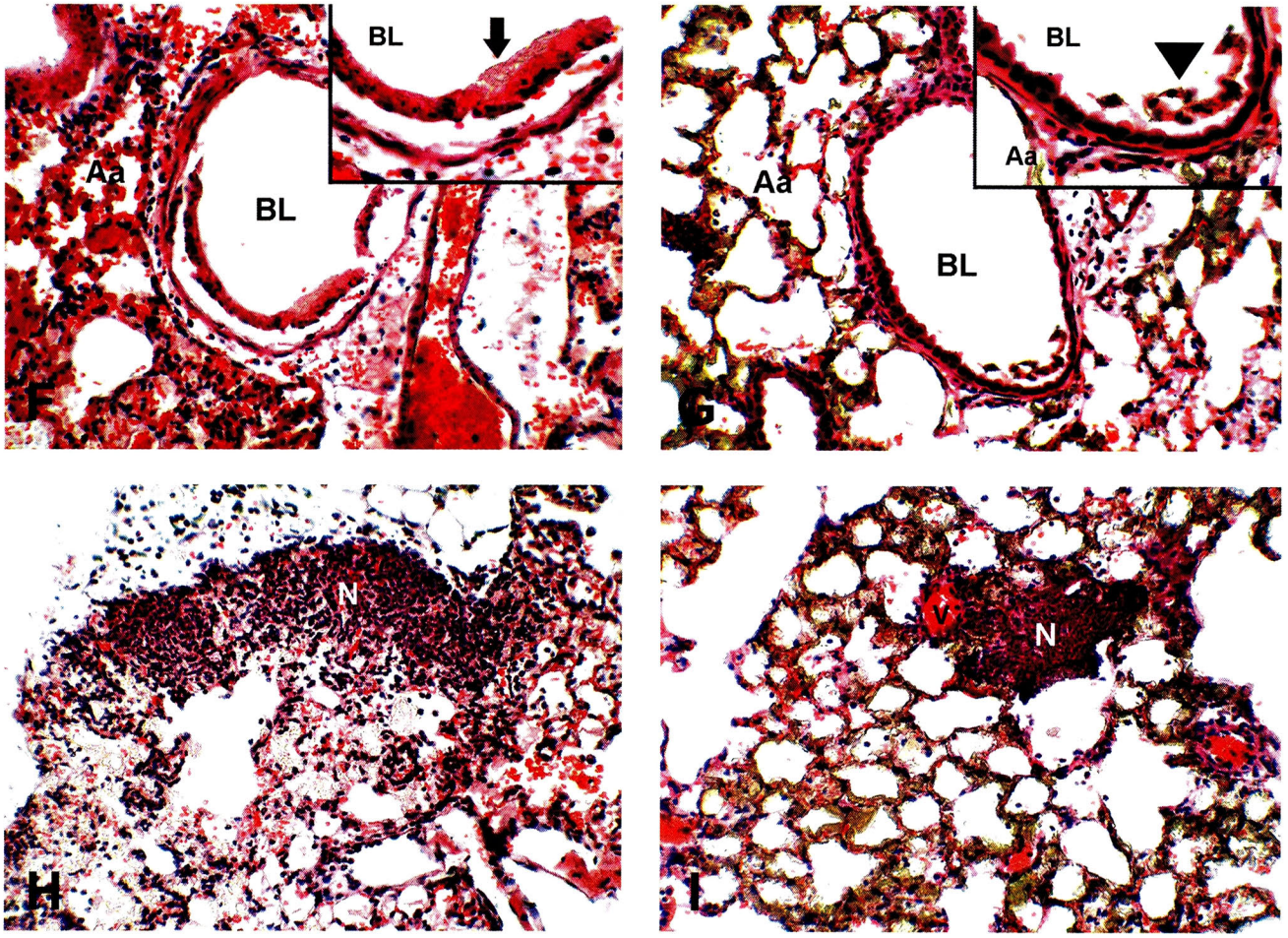
BL
Aa
BL
F
BL
Aa
Aa
BL
G
N
H
V
N
I

Figure 3. Photomicrographs from the lungs of mice. H&E stain. (A) No inflammatory changes were observed in the lung from the control groups. 120×. (B) UFCSs treated mice sacrificed at 30 min after exposure show more severe congestion and hemorrhage than those in FCSs treated animals (C). FCSs particles (solid arrow) accumulated in alveolar lumen. (B), (C) 390×. Mice sacrificed at 2 hr after instillation with UFCSs (D) or FCSs (E). Attenuated bronchiolar epithelial cells were seen in both treatment groups. (D), (E) 190×. *Inset:* Higher magnification of bronchiolar epithelial cell attenuation with UFCSs (solid arrow) or FCSs (arrowhead) on epithelial surfaces. 800×. (F) UFCSs treated mice sacrificed at 12 hr after exposure. Marked necrosis and desquamation of bronchiolar epithelial cells were seen. 190×. UFCSs particles (solid arrow) accumulated on necrotic and desquamated epithelial cells were also observed (inset: 750×), compared to (G) FCSs treated mice. Moderate bronchiolar epithelial cell degeneration and subsequent desquamation were seen. 190×. *Inset:* Higher magnification of bronchiolar epithelial cell degeneration with some desquamated epithelial cells (arrowhead). 750×. (H) UFCSs treated mice sacrificed at 24 hr after exposure. Marked infiltration of neutrophils with some inflammatory nodules (N) in alveolar air spaces was seen. 190×. (I) Moderate neutrophil infiltration with a small inflammatory nodule (N) adjacent to the blood vessel (v) was observed in FCSs treated mice. 190×. BL = bronchiolar lumen; Aa = alveolar air space.

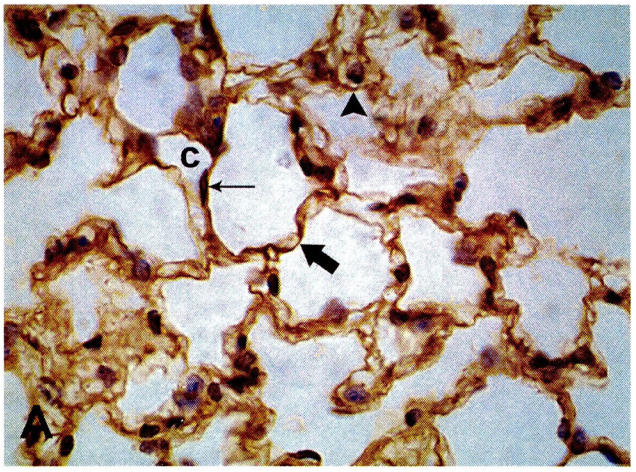
C
A

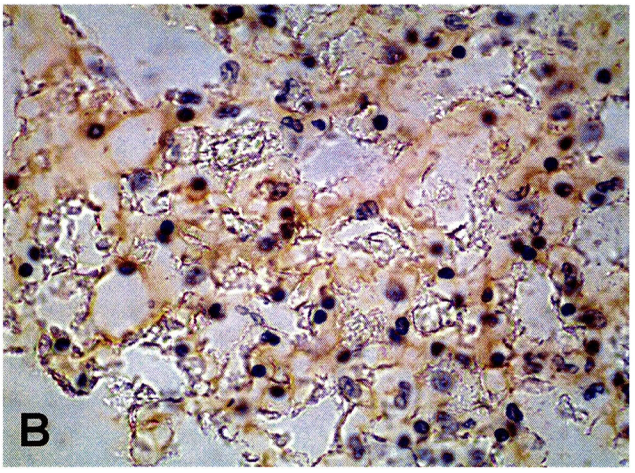
B

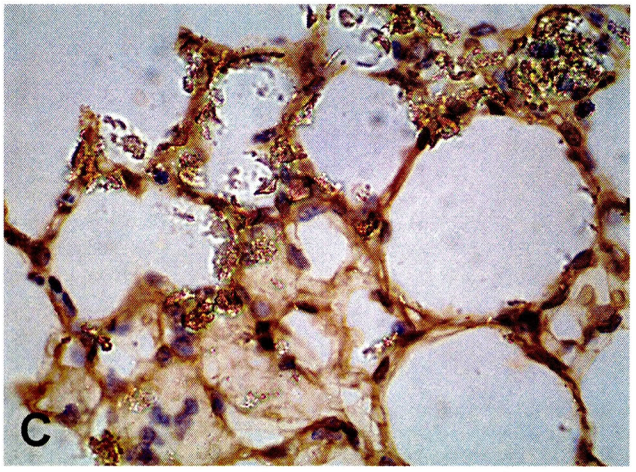
C

Figure 4. Laminin immunohistochemistry in lungs of mice sacrificed at 24 hr after instillation with Milli-Q® purified water, UFCSs and FCSs. (A) Brown faint string-like staining patterns along basement membranes (solid arrow). UFCSs and FCSs treated mice show weakly positive discontinuities in the basement membranes of alveoli; weaker positivity and more discontinuous pattern of alveolar basement membranes were observed in UFCSs treated animals (B) compared to FCSs treated animals (C). Arrow indicates alveolar capillary endothelial cells. c: alveolar capillary lumen. (A), (B), (C) 580×.

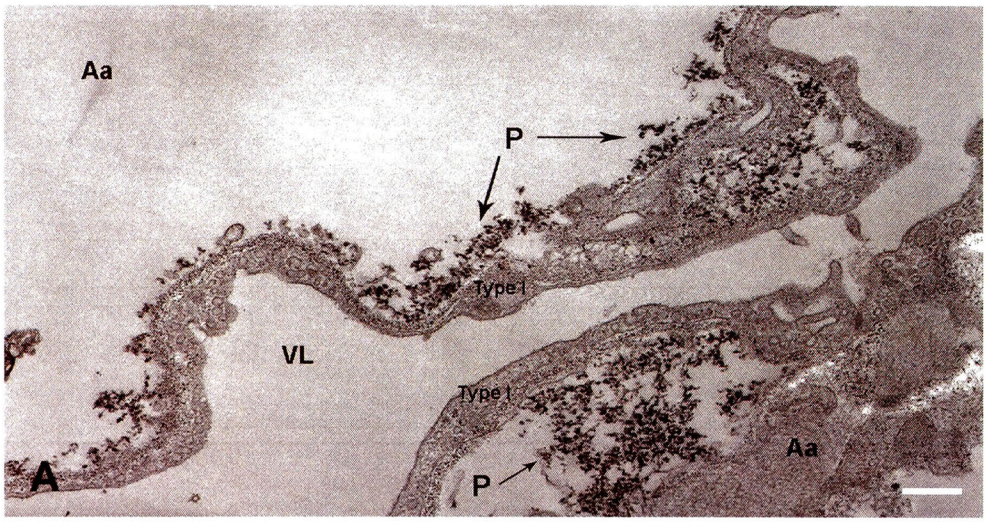
Aa
P
Type I
VL
Type I
Aa
P
A

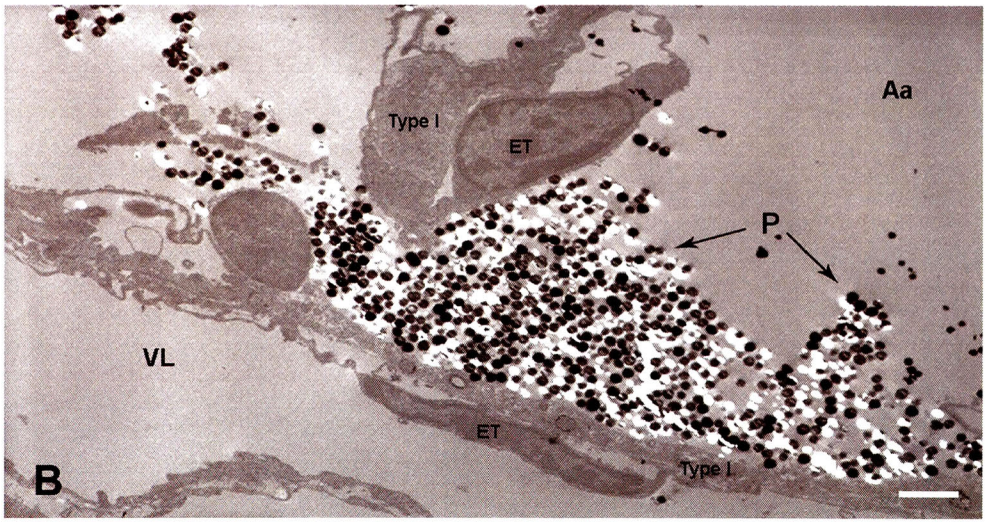
Aa
Type I
ET
P
VL
ET
Type I
B

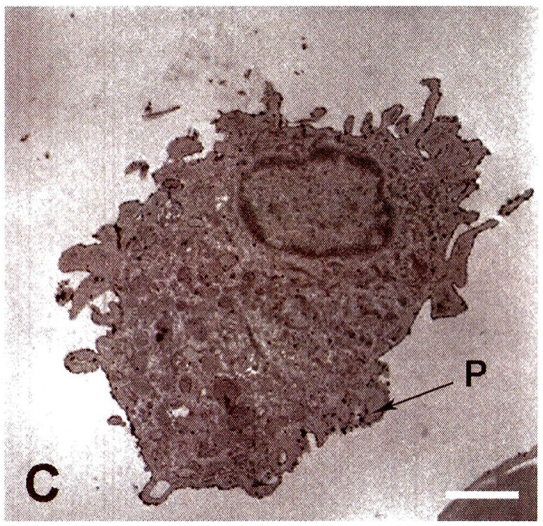
P
C

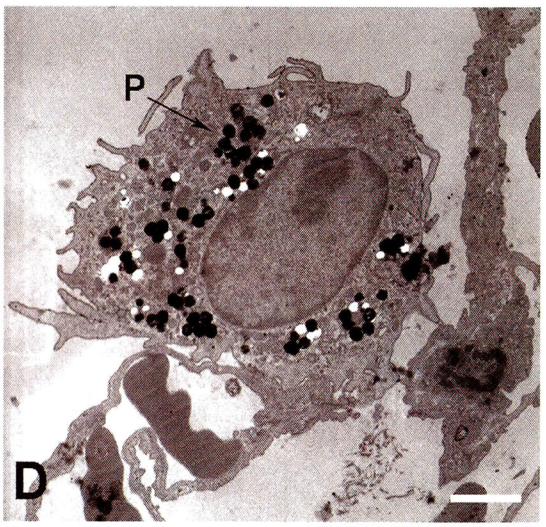
P
D

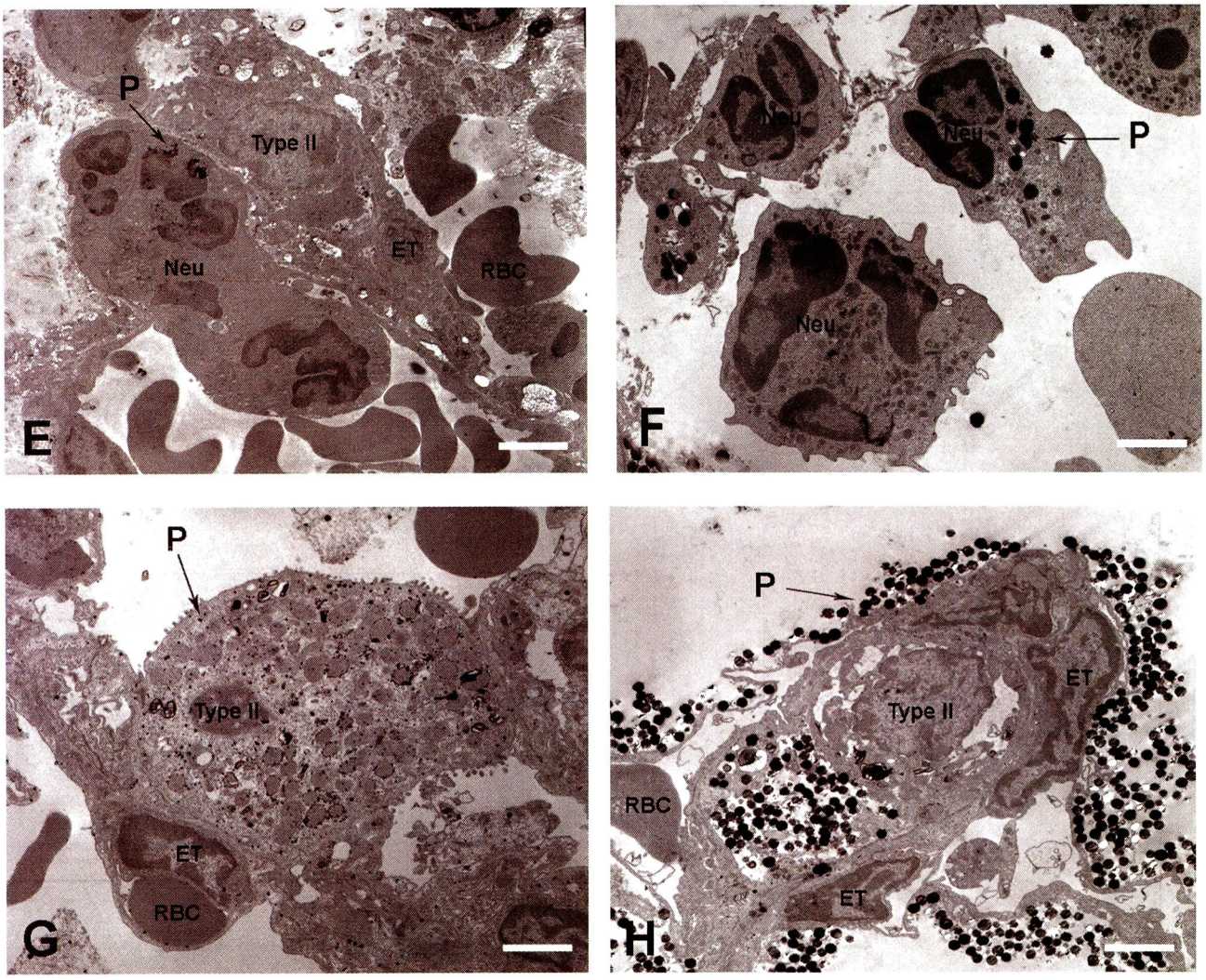
P
Type II
Neu
ET
RBC
E
Neu
Neu
P
Neu
F
P
Type II
ET
RBC
G
P
ET
Type II
RBC
ET
H

Figure 5. Ultrastructure of the distribution of particles in the lungs from various time points. Numerous free and aggregate forms of particles along the apical surface of the plasma membrane of alveoli in both UFCSs (A) and FCSs (B) treated animals killed at 24 hr post-exposure. Bar = 100 nm. Particle-laden AMs showing round or polygonal shapes with numerous lysosomes, phagolysosomes, and aggregated UFCSs (C) or FCSs (D) particles in their cytoplasms., 12 hr post-exposure, bar = 200 nm. Instilled UFCSs (E) or FCSs (F) particles in the cytoplasm of neutrophils around the sites of inflammatory lesions., 12 hr post-exposure, bar = 200 nm. Accumulation of UFCSs (G) or FCSs (H) particles in the cytoplasm of hyperplastic type II alveolar epithelial cells., 24 hr post-exposure, bar = 200 nm. Aa: alveolar air space, ET: alveolar endothelial cell, Neu: neutrophil, RBC: red blood cell, Type I: type I alveolar epithelial cell, Type II: type I alveolar epithelial cell, P: particles, VL: vascular lumen.

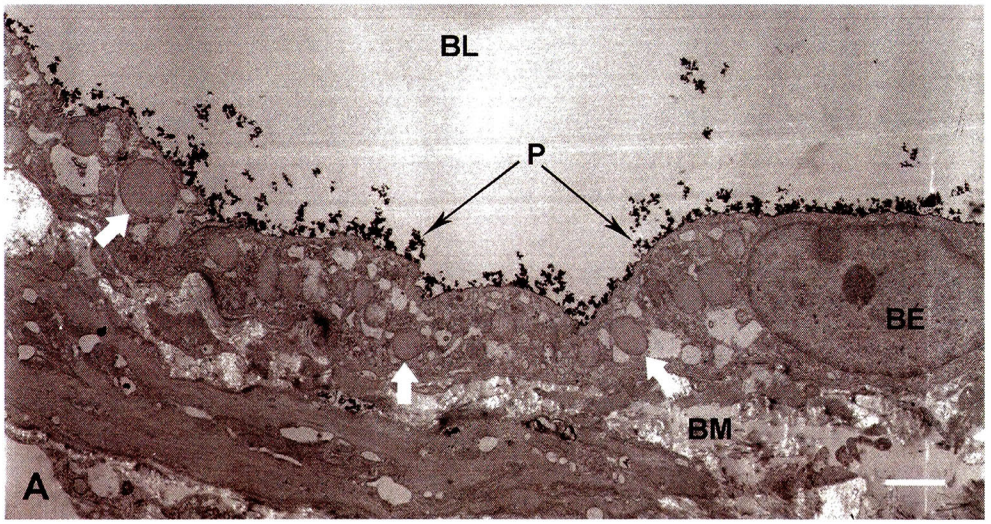
BL
P
BE
BM
A

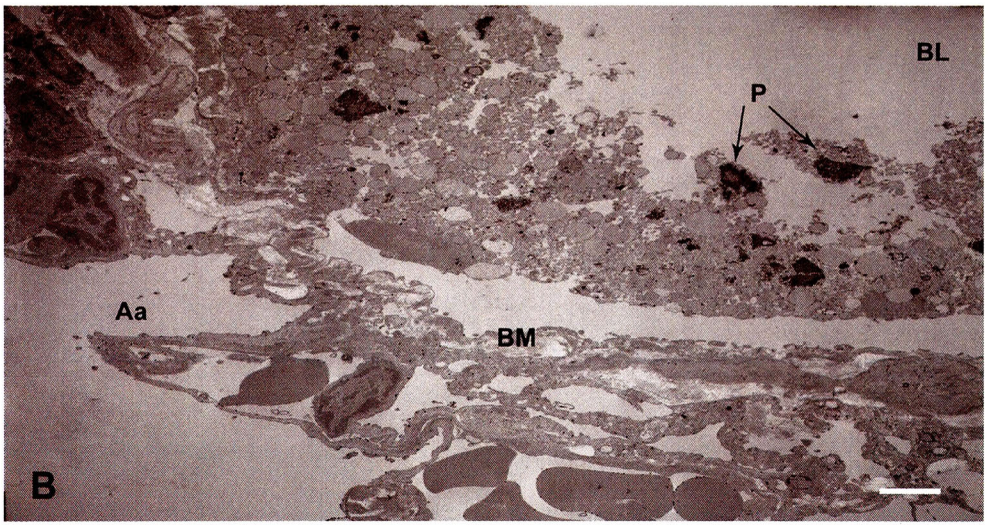
BL
P
Aa
BM
B

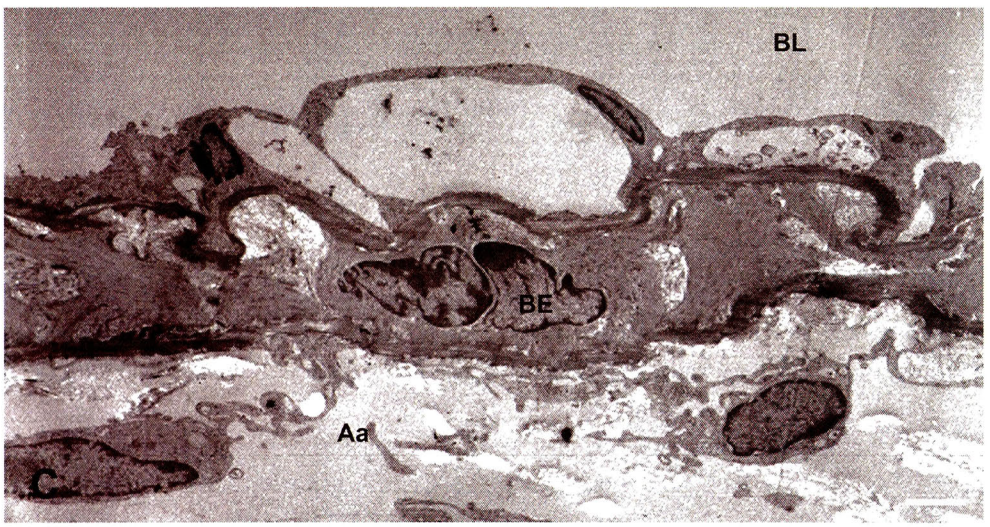
BL
BE
Aa
C

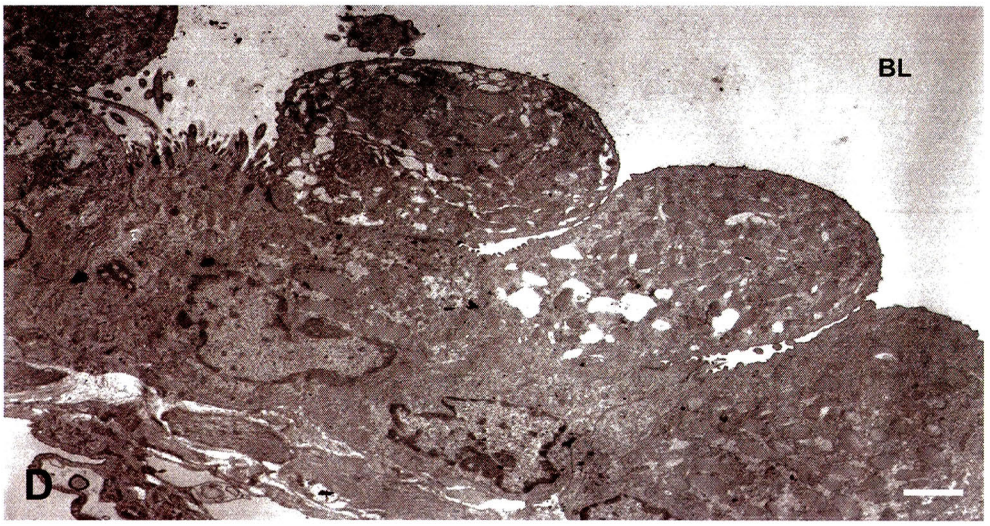
BL
D

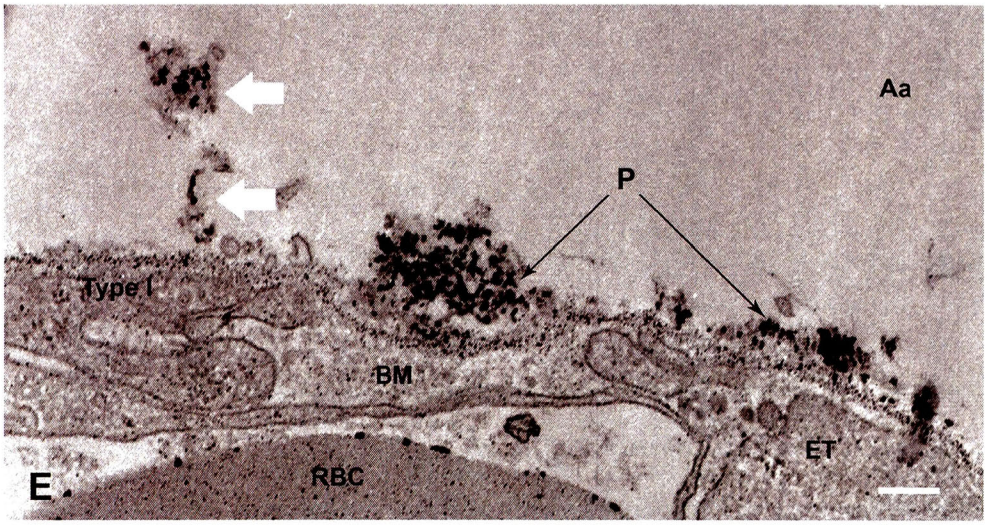
Aa
P
Type I
BM
ET
RBC
E

Figure 6. Transmission electron microscopy of lungs from UFCSs treated mice killed at 12 hr post-exposure. (A) Bronchiolar epithelial cells showing severe destructive changes including marked swelling of endoplasmic reticulum (white solid arrows) with accumulated UFCSs particles (black arrows) on their surface and thickened bronchiolar basement membranes. Bar = 1.54 μm. (B) Desquamation of necrotic bronchiolar epithelial cells with aggregated UFCSs particles (black arrows) and basement membrane dissociation. Bar = 2.4 μm. (C) Vacuolation of bronchiolar epithelial cells. Bar = 1.5 μm. (D) Clara cells showing numerous mitochondria, irregular sER and remarkable edema in the cytoplasm. Bar = 1.5 μm. (E) Aggregates of UFCSs particles (black arrows) attaching on the surface of the denuded basement membrane and remnants of desquamated necrotic alveolar epithelial cells (white solid arrows). Bar = 200 nm. Aa: alveolar air space, BM: basement membrane, ET: alveolar endothelial cell, BE: bronchiolar epithelial cell; BL: bronchiolar lumen, RBC: red blood cell, Type I: type I alveolar epithelial cell, P: UFCSs particles.

CHAPTER 2

Acute and Subacute Pulmonary Toxicity of Low Dose of Ultrafine Colloidal Silica Particles in Mice after Intratracheal Instillation

Abstract

To study the acute and subacute lung toxicity of low dose of ultrafine colloidal silica particles (UFCSs), mice were intratracheally instilled with 0, 0.3, 3, 10, 30 or 100 μg of UFCSs. Cellular and biochemical parameters in bronchoalveolar lavage fluid (BALF), histological alteration and the body weight were determined at 3 days after instillation. Exposure to 30 or 100 μg of UFCSs produced moderate to severe pulmonary inflammation and tissue injury. To investigate the time response, mice were instilled with 30 μg of UFCSs and sacrificed at intervals from 1 to 30 days post-exposure. UFCSs induced moderate pulmonary inflammation and injury on BALF indices at acute period; however, these changes gradually regressed until recovery during the experiment. Concomitant histopathological and laminin immunohistochemical findings generally correlated to BALF data. TUNEL analyses in UFCSs-treated animals showed a significant increase of the apoptotic index in lung parenchyma at all observation times. 8-OHdG expression occurred in lung epithelial cells and activated macrophages, which correlated to lung lesions in UFCSs-treated mice. These findings suggest that instillation of a small dose of UFCSs causes transient acute moderate lung inflammation and tissue damage. Oxidative stress and apoptosis may underlie the lung tissue injury induction.

Keywords: apoptosis, bronchoalveolar lavage, intratracheal instillation, lung toxicity, oxidative stress, ultrafine colloidal silica.

Introduction

Colloidal silica, one of synthetically made amorphous silica that became widely used in many industries and available for various applications, is known to be far less active in producing pulmonary damage when compared to crystalline silica (Warheit et al., 1995). Subchronic inhalation toxicity studies in rats on colloidal silica reported that inhalation exposure of 50 mg/m^3 (2418 μg/lung) or 150 mg/m^3 (7378 μg/lung) Ludox® colloidal silica , 2.9-3.7 μm of mass median aerodynamic diameter (MMAD) ranges, produced transient pulmonary inflammatory responses. The severity and incidence of pulmonary lesions decreased progressively after a 3-month recovery period. The no-observable-effect level (NOEL) was 10 mg/m^3 (489 μg/lung) (Lee and Kelly, 1992; Warheit et al., 1991).

Many toxicological studies made it clear that ultrafine particles (diameter < 100 nm) of various types can cause lung inflammatory responses, epithelial cell hyperplasia, inhibit phagocytosis, increased chemokine expression, lung fibrosis, increased oxidant-generating abilities, and lung tumors (Brown et al., 2000; Donaldson and MacNee, 2001; Warheit, 2004). Ultrafine particles have been shown to have a greater inflammatory lung responses and the development of particle-mediated lung diseases than the fine particles per given mass (Li et al., 1999; Nemmar et al., 2003). In the first chapter, we have described acute pulmonary pathological effects caused by single intratracheal exposure to colloidal silica and compared the size effects in light and electron microscopy in mice. Our results showed that intratracheal instillation of high dose (3 mg/lung) of colloidal silica caused severe acute pulmonary inflammation and tissue injury; ultrafine colloidal silica particles (UFCSs) induced more severe changes than fine colloidal silica particles (FCSs). The UFCSs used in

our study had a primary particle diameter of 14 nm and 10 – 150 nm of particle size distribution ranges in the lung. Moreover, the surface area of UFCSs was almost fifteen times greater than FCSs (Kaewamatawong et al., 2005). The increased toxicity of ultrafine particles can be related to their greater surface area per given mass, high number concentration, surface property, chemical composition and unique deposition in the lung (Brown et al., 2001; Jaques and Kim, 2000; Oberdorster, 2001; Pandurangi et al., 1990). Moreover, reactive oxygen species (ROS) also play an important role in ultrafine particle-induced pulmonary damage (Gilmour et al., 1997).

The aim of this study was to clarify biological and pathological events of intratracheally instilled low dose of UFCSs on the lungs of mice during the acute and subacute stages using BAL techniques and histopathological evaluations. In addition, factors that could be important in the induction of pulmonary toxicity of UFCSs were investigated with the use of immunohistochemistry.

Materials and Methods

Experimental animal

Male ICR mice, weighing 35-38 g and 7-8 weeks of age, were purchased from CLEA Japan, INC. The mice were housed in an animal facility under 12/12 hr light/dark cycle, temperature of 24 ± 1 °C, relative humidity of 55 ± 10% and negative atmospheric pressure. They were provided with mouse chow and filtered tap water *ad libitum* throughout the experiment. All animal experiments were performed according to the National Institute for Environmental Studies Guidelines for Animal Welfare.

Particles

Ultrafine colloidal silica (Grade PL-1) was obtained as a gift from Fuso Chemical Co.,Ltd.,Japan (Lot No. R2Z007). The silica particles had a spherical configuration with a relatively uniform size distribution averaging approximately 14 nm. The surface area, which measured by Brunauer, Emmett and Teller (BET) method, was 194 m^2/g. The UFCSs had very low levels of metal compositions (potassium, aluminium, magnesium < 0.01 ppm; Iron < 0.005 ppm; sodium = 0.05 ppm; calcium < 0.01 ppm) (Kaewamatawong et al., 2005). The silica particles were suspended in water at a concentration of 120 mg/ml and then sterilized at 0.5 kgf/cm^2 and 120 °C for 20 min.

Experimental design

***Dose response*:** Sixty mice were divided randomly into 6 groups of 10 animals each. The mice were anesthetized by intraperitoneal (IP) injection of 3 mg/kg xylazine (2% solution, Celactal®; Bayer, Tokyo, Japan) and 75 mg/kg ketamin (Ketalar® 50, Sankyo, Tokyo, Japan). 50 µl aqueous suspensions of 0.3, 3, 10, 30 or 100 µg of UFCSs suspended in

0.01 M phosphate-buffered saline (PBS) were instilled intratracheally via a small canule, followed by 0.1 ml of air. After intratracheal instillation, the mice were kept in an upright position for 15 min to allow the fluid to spread throughout the lung. The control groups of mice were instilled with 50 µl of 0.01 M PBS.

***Time effect*:** Eighty mice were divided randomly into 10 groups of 7-9 animals each. The mice were intratracheally instilled with 50 µl of 30 µg of UFCSs suspended in 0.01 M PBS as described above. The control groups of mice were instilled with 50 µl of 0.01 M PBS. Animals in each group were killed at 1, 3, 7, 15 and 30 days after instillation, respectively.

Bronchoalveolar lavage

The trachea was exposed with a midline incision and cannulated with a modified 21 gauge needle. Bronchoalveolar lavage (BAL) was accomplished by 3 × 1 ml sterile 0.01 M PBS. The recovery of BALF for each mouse was measured, and the recovery rate was calculated. The average fluid recovery was greater than 90%. The BALF was centrifuged at 8,000 rpm for 8 min at 4 °C and the supernatants were stored at -80 °C until analysis.

Biochemical and cytological evaluation of BALF

The first tubes of BAL supernatant were used to measure total concentration of protein using the micro-BCA method (Pierce Chemical Co. Rockford, IL). BALF cells were quantified by hemocytometric counting, and cell viability was determined by exclusion of tryphan blue dye. Cell differentiation was evaluated for BALF pooled from each mouse by Diff-Quik stain (Sysmex®, Kobe, Japan).

Histopathology

After gross examination of respiratory organs such as lungs and hilar lymph nodes, the lungs and trachea were removed *en bloc* and instilled with 10% buffered neutral formalin. Whole lungs and hilar lymph nodes were processed according to routine histological techniques. After paraffin embedding, 3 μm sections were cut and stained with hematoxylin and eosin (H&E) and Azan stain.

Immunohistochemistry:

Laminin: Tissue sections from lung were immunostained by using avidin-biotin complex (ABC) method, in which labeled Streptavidin biotin (LSAB) kit (DAKO, Glostrup, Denmark) was included. After deparaffinization of the sections, the sections were treated with proteinase K for 30 min at 39 °C. The sections were incubated with 3% H_2O_2 to quench endogenous peroxidase for 15 min at room temperature and then with 10% normal goat serum for 5 min in microwave oven 250 w to inhibit nonspecific reactions. Thereafter the sections were reacted over night at 4 °C with Rabbit anti-laminin monoclonal antibody diluted 1:200 (DAKO, Glostrup, Denmark). The peroxidase conjugated goat anti-rabbit IgG diluted 1:400 (DAKO) was reacted to sections as a secondary antibody in microwave oven 200 w for 7 min. The positive reactions resulted in brown staining with the substrate 3,3'-diaminobenzidine tetrahydrochloride (DAB), and the sections were counterstained with hematoxylin for 30 sec.

8-hydroxy-2-deoxyguanosine (8-OHdG): After deparaffinization and rehydration, sections were pretreated with 3% hydrogen peroxide in absolute methanol for 10 min and then washed with PBS. Non-specific background was eliminated by incubating the sections with Reagent 1A (ZYMED® LAB-SA SYSTEM HISTOMOUSE™ –PLUS KITS) for 30 min

and rinsed well with distilled water (DW). The section were incubated with Reagent 1B (ZYMED® LAB-SA SYSTEM HISTOMOUSE™ –PLUS KITS) for 10 min and rinsed well with DW and PBS. 8-OHdG monoclonal antibody (Japan Institute for the Control of Aging, Shizuoka, Japan) (1:200 in PBS) was incubated for 1 hr on the tissue. The section were washed with PBS and incubated with biotinylated secondary antibody, Reagent 1C (ZYMED® LAB-SA SYSTEM HISTOMOUSE™ –PLUS KITS) for 30 min and then washed with PBS. Streptavidin-peroxidase, Reagent 2 (ZYMED® LAB-SA SYSTEM HISTOMOUSE™ –PLUS KITS) was then added to the section for 20 min. The sections were washed with PBS. The peroxidase activity was visualized by addition of substrate-chromogen solution, Reagent 3 (ZYMED® LAB-SA SYSTEM HISTOMOUSE™ –PLUS KITS). Peroxidase will catalyze the substrate (hydrogen peroxidase) and convert the chromogen (AEC) to a red deposit, which demonstrates the location of the antigen. The section were rinsed in DW and counterstained with hematoxylin, Reagent 4 (ZYMED® LAB-SA SYSTEM HISTOMOUSE™ –PLUS KITS) for 30 sec.

Detection of apoptosis

The lung and hilar lymph node tissues fixed in 10% neutral buffered formalin and embedded in paraffin were processed for a Terminal Deoxynucleotidyl Transferase Biotin-dUTP Nick End Labeling (TUNEL) assay. Apop Tag® Peroxidase *In situ* Apoptosis Detection Kit (Chemicon International, Temecula, CA) was used following the manufacturer's instruction. Briefly, the slides were pretreated with proteinase K, applied to H_2O_2 and incubated with the reaction mixture containing Terminal Deoxynucleotidyl Transferase (TdT) and digoxigenin-conjugated dUTP for 1 hr at 37 °C. Labeled DNA was visualized with peroxidase-conjugated anti-digoxigenin antibody with DAB as the

chromogen and then counterstained the slides with hematoxylin for 30 sec. Apoptotic cells were identified by TUNEL in conjunction with characteristic morphological changes, such as cell shrinkage, membrane blebbing, and chromatin condensation, to distinguish apoptotic cells and apoptotic bodies from necrotic cells. For each sample, 1000 cells/organ were examined and scored at a magnification of ×400. The results represented apoptotic index indicating percentages of cells affected by apoptosis.

Statistical analysis

Data were expressed as means ± standard error (SE). Statistical analysis was evaluated using Student's t-test. Differences between means were regarded as significant at p value of less than 0.05.

Results

Dose response

***Body weight*:** The body weights of mice after instillation with UFCSs 0.3 and 10 μg significantly decreased on day 1, and then increased from 2 days after instillation. In mice exposed to 30 and 100 μg UFCSs, body weight was significantly decreased compared to controls throughout 3 days post-exposure (Figure 1).

***Bronchoalveolar lavage fluid analysis*:** Table 1 presents the results for cellular and biochemical constituents in BALF after instillation of various doses of UFCSs. The total cell numbers in BALF were significantly increased after 3 days post-exposure for 10, 30 and 100 μg UFCSs-exposed groups. Cell differential analyses of BALF of mice exposed to 30 and 100 μg UFCSs demonstrated significant increases in the numbers of neutrophils and lymphocytes at 3 days after instillation. Total protein value in lung lavage fluid is considered to be a sensitive marker of alterations in the permeability of alveolar-capillary barrier. All exposure groups showed significant increase in total protein values in BALF above controls following a 3-day post-exposure.

Histopathology: Histopathological changes (Data not shown) induced by intratracheal instillation of 30 or 100μg at 3 days post-exposure showed moderate to severe focal alveolitis especially at the terminal bronchiolar and alveolar duct regions. In the foci, infiltration and accumulation of numerous particle-laden alveolar macrophages (AMs), neutrophils and fewer lymphocytes were observed. Increasing numbers of active AMs and neutrophils in alveolar spaces were also observed together with swelling and regenerative hyperplasia of type II epithelial cell. The other lower doses (0.3, 3 and 10μg) of UFCSs

induced similar histopathological patterns. However, the lesions were milder and occupied a small area of the lung specimens.

Table 1. Changes in bronchoalveolar lavage fluid contents in mice at 3 days after intratracheal instillation of ultrafine colloidal silica particles (Mean ± SE; n = 6-7)

Dose	Total cells ($\times 10^5$)	Macrophages ($\times 10^5$)	Neutrophils ($\times 10^5$)	Lymphocytes ($\times 10^5$)	Total protein (μg/ml)
0	2.19 ± 0.37	2.1 ± 0.32	0.01 ± 0.01	0.05 ± 0.03	170.8 ± 12.79
0.3	3.08 ± 0.99	2.81 ± 0.89	0.14 ± 0.09	0.12 ± 0.04	318.85 ± 57.79*
3	2.54 ± 0.45	2.4 ± 0.37	0.03 ± 0.02	0.1 ± 0.07	236.86 ± 12.81*
10	3.81 ± 0.38*	3.64 ± 0.35*	0.05 ± 0.02	0.1 ± 0.03	257.99 ± 30.74*
30	4.99 ± 0.46*	3.61 ± 0.58*	1.19 ± 0.28*	0.17 ± 0.04*	799 ± 69.82 *
100	5.30 ± 0.67*	2.6 ± 0.44	1.93 ± 0.42*	0.76 ± 0.23*	1804.41 ± 264.38*

* Significantly different from the control group; $p < 0.05$

Time effect

***Body weight*:** Body weights were collected daily from 1 day after exposure through the end of the post-exposure period. A significant decrease in body weight was noted in the exposure groups compared to the control groups from 1 day after instillation, and then recovery occurred over the next 5 days post-exposure (Figure 2).

***Bronchoalveolar lavage fluid analysis*:** Following instillation of 30 μg UFCSs, the numbers of total cells, macrophages, neutrophils and lymphocytes in BALF at 1, 3, 7, 15 and 30 days post-exposure showed a transient increase pattern and then returned toward control levels (Table 2). Total numbers of lung cells were significantly increased and persisted up to 15 days before returning to control levels by 30 days post-exposure.

Significantly elevated numbers of AMs were evident at 1 day after instillation and remained significant increased for over 7 days. The numbers of neutrophils increased markedly 1 day after instillation, followed by a further increase over 3 days. Lymphocytes showed a changing pattern different from the other inflammatory cells. Significant differences over corresponding controls of lymphocytes were gradual increase over the 7 days of the experiment and then returned to control levels by 30 days post-exposure (Table 2).

The concentrations of total protein in BALF in UFCSs-treated mice were greater than those of control animals at 1 day after exposure and gradually returned to control levels at 15 days post-exposure (Table 2).

***Histopathology*:** In the controls, no significant lesions were observed in all time points (Figure 3A). By contrast, at 1 day after instillation, moderate increases of neutrophils sharply demarcated from the remaining normal alveoli were noted in UFCSs treated groups. A number of nodular aggregates of neutrophils and particle-laden AMs were observed in some alveolar regions adjacent to the bronchioles. The nodular lesions consisted of neutrophils, active AMs, particle-laden AMs and some cell debris (Figure 3B). Thickened alveolar wall with increased number of inflammatory cells was also seen. By 3 days after instillation, moderate focal alveolitis characterized by accumulation of numerous particle-laden AMs, neutrophils and fewer lymphocytes was observed at the terminal bronchiolar and alveolar duct regions (Figure 3C). Alveolar septal walls surrounding the foci were thickened with occasional type II epithelial cell regenerative hyperplasia. Particle-laden AMs and neutrophils infiltration into bronchial associated lymphoid tissue (BALT) was also observed. Changes in the lungs of mice killed at 7 days after UFCSs instillation were

restricted to the appearance of the aggregated foci consisting of particle-laden AMs, lymphocytes and fibroblasts with occasional deposition of minimal volume of collagen fibers (Figure 3D). The lesions were located around blood vessels adjacent to terminal bronchioles and alveolar ducts. Peribronchiolar and perivascular lymphoid proliferation was present. The hilar lymph nodes were slightly enlarged associated with accumulation of particle-laden macrophages and hyperplastic histiocytes in subcapsular and medullary sinus.

At 15 days post-exposure, the inflammatory foci in lung parenchyma were markedly reduced in number and more focally concentrated, which were characterized by loose accumulation of particle-laden AMs, lymphocytes and fibroblasts with increased collagen fiber deposition (Figure 3E). Some alveolar walls enclosing to the foci were thickened due to hyperplasia of type II epithelial cells and interstitial accumulation of macrophages. Peribronchiolar and perivascular lymphoid tissues which were activated at the acute stage showed inactive structure. In 30 days after instillation, inflammatory lesions of lung and lymph node were almost recovered except for slight thickening of alveolar septal walls with some areas of interstitial fibrosis (Figure 3F).

Table 2. Changes in bronchoalveolar lavage fluid contents in mice up to 30 days after intratracheal instillation of ultrafine colloidal silica particles (Mean ± SE; n = 5-8)

Days	Groups	Total cells ($\times 10^5$)	Macrophages ($\times 10^5$)	Neutrophils ($\times 10^5$)	Lymphocytes ($\times 10^5$)	Total protein (μg/ml)
1	Control	2.36 ± 0.39	2.34 ± 0.35	0.001 ± 0.001	0.01 ± 0.003	165.46 ± 10.47
1	UFCSs	6.3 ± 0.2*	4.39 ± 0.48*	1.96 ± 0.41*	0.04 ± 0.01*	1037.66 ± 121.09*
3	Control	2.08 ± 0.23	2.05 ± 0.22	0.005 ± 0.003	0.02 ± 0.01	171.94 ± 15.78
3	UFCSs	4.99 ± 0.56*	3.58 ± 0.54*	1.27 ± 0.31*	0.13 ± 0.04*	734.73 ± 117.21*
7	Control	2.16 ± 0.02	2.14 ± 0.01	0.0 ± 0.0	0.02 ± 0.01	216.56 ± 23.86
7	UFCSs	4.35 ± 0.28*	3.82 ± 0.32*	0.06 ± 0.05	0.46 ± 0.18*	327.78 ± 32.53*
15	Control	1.54 ± 0.22	1.52 ± 0.22	0.0 ± 0.0	0.02 ± 0.01	179.94 ± 14.66
15	UFCSs	2.92 ± 0.53*	2.72 ± 0.5	0.003 ± 0.003	0.2 ± 0.08*	210.86 ± 12.19
30	Control	2.67 ± 0.44	2.64 ± 0.45	0.008 ± 0.007	0.02 ± 0.01	247.95 ± 31.38
30	UFCSs	3.74 ± 0.32	3.65 ± 0.29	0.0 ± 0.0	0.08 ± 0.04	230.56 ± 37.13

* Significantly different from the control group; $p < 0.05$

Immunohistological evaluation

Laminin: Thin string-like lines of intense brown positive stains were observed in bronchial basement membrane, blood vessel basement membrane, around bronchial gland and along alveolar septa of mice from control groups (Figure 4A). Lung tissues from UFCSs-treated mice at 1, 3 and 7 days after instillation showed extensive patchy areas of non-stain or weak positive reaction; the basement membranes of the alveoli in site of the inflammatory foci showed interruptions with a patchy distribution of the immunoreactivity (Figure 4B). Lung tissues from UFCSs-treated mice at 15 and 30 days after instillation showed mostly

similar positive pattern as in the controls. However, brown faint discontinuous lines were observed in the areas of alveolar wall thickening (Figure 4C).

TUNEL assay: Table 3 presents the percentage of apoptotic positive cells in bronchiolar epithelium and lung parenchyma of five animals belonging to each experiment groups. No significant differences in the apoptotic index in bronchial epithelial cells between control and UFCSs-exposed groups except for transient increase at 3 days after instillation. Whereas the average numbers of apoptotic cells in lung parenchyma of exposure animals were significantly elevated above the controls at all time points examined. TUNEL pictures

8-OHdG: In control lungs, the immunohistochemical staining of 8-OHdG was barely detectable in both airway epithelium and lung parenchyma (Figure 5A). By contrast, in the UFCSs-treated mice at 1 day post exposure, positive staining for 8-OHdG appeared in a large number of cells associated with pulmonary inflammation. 8-OHdG was expressed mainly in the cytoplasm and partially in the nuclei of bronchiolar epithelial cells, alveolar epithelial cells and activated AMs (Figure 5B). After 3 and 7 days, 8-OHdG was observed chiefly in macrophages located around the sites of focal alveolitis but minimally in bronchiolar and alveolar epithelial cells (Figure 5C). At 15 and 30 days post-exposure, a cytoplasmic expression of 8-OHdG was only present in a small number of alveolar epithelial cells (Figure 5D).

Table 3. Immunohistochemical assessment of apoptosis (apoptotic index) in lung sections of control and 30 μg UFCSs-treated mice (Mean ± SE; n = 5)

Days after instillation	Apoptotic index (%) in bronchial epithelium		Apoptotic index (%) in lung parenchyma	
	Control	30 μg UFCSs	Control	30 μg UFCSs
1	0.86 ± 0.25	1.06 ± 0.18	0.1 ± 0.04	1.0 ± 0.31*
3	0.28 ± 0.04	0.62 ± 0.15*	0.12 ± 0.05	0.66 ± 0.14*
7	0.4 ± 0.25	0.72 ± 0.23	0.04 ± 0.02	1.46 ± 0.19*
15	0.86 ± 0.31	1.46 ± 0.40	0.18 ± 0.15	1.0 ± 0.20*
30	1.12 ± 0.48	2.02 ± 1.00	0.06 ± 0.02	0.58 ± 0.05*

* Significant different from the control group; $p < 0.05$

Discussion

The purpose of this study was to determine the biological and pathological effects of intratracheally instilled low dose of UFCSs on the lungs of mice in terms of dose and time response during the acute and subacute stages. To study dose response, we exposed mice to different doses of UFCSs and investigated the changes in body weight, inflammatory cellular and biochemical parameters in BALF, and histopathology at 3 days after instillation. The results showed that instillation of 30 or 100 μg UFCSs produced moderate to severe pulmonary effects consistent with the development of lung injury, as evidenced by increased total cells, together with increases in leukocyte counts in BALF. This was accompanied by change in alveolar permeability, as measured by total protein in lavage fluid. To investigate time effect, bronchoalveolar lavage fluid analysis was carried out from 1 day through 30 days after a single instillation of 30 μg UFCSs. The effects of UFCSs on bronchoalveolar lavage indices suggested that UFCSs induced moderate pulmonary inflammation and injury at an early stage, but this effect gradually decreased during the experiment. Concomitant histopathological findings generally correlated to BALF data, showing moderate pulmonary inflammation and injury characterized by infiltration of neutrophils and active AMs, focal alveolitis, particle-laden AMs accumulation, and thickened alveolar wall with occasional regenerative hyperplasia of type II epithelial cells at day 1, 3 and 7 after instillation. However, the lung lesions were milder at 15 days and almost recovered at the final time point.

Subchronic inhalation toxicity studies in rats demonstrated that exposure to colloidal silica at the concentration of 50 mg/m^3 (2418 μg/lung) or 150 mg/m^3 (7378

μg/lung) induced transient pulmonary inflammation but changes may regress during the recovery period compared to persistent pulmonary inflammation by crystalline silica, while no toxic pulmonary effects were measured in animals exposed to 10 mg/m^3 (489 μg/lung). The range of airborne particle sizes, in the form of MMAD was 2.9-3.7 μm (Lee and Kelly, 1992; Warheit et al., 1991). In our study, we exposed mice with a single intratracheal instillation of various low doses of UFCSs. Our data showed that even a small dose (30 μg/lung) of UFCSs can induce acute moderate pulmonary inflammation and injury characterized by increased cellular and biochemical indices in BALF with concomitant progressive histopathological lesions. However, these inflammatory responses receded and recovered during the experiment. From the results of dose responses, pulmonary lesions and significant differences from the controls for BALF total protein were still observed in mice exposed to 0.3, 3 or 10 μg UFCSs. Thus, the concentration that can induce no toxic pulmonary effects in our study might be less than 0.3 μg/lung.

Laminin, a noncollagenous glycoprotein with an approximate molecular weight of 900000, is an intrinsic component of all basement membranes. Laminin plays a central role in the formation, the architecture, and the stability of basement membranes as well as control of cellular interactions. Because it is present in all pulmonary basement membranes, it can be used as a marker for these structures (Aumailley and Smythe, 1998; Gil and Hernandez, 1984). In mice exposed to UFCSs, weak and discontinuous positive stainings of laminins were observed along basement membranes in both airway epithelium and lung parenchyma especially in the site of the inflammatory foci. The distribution of the basement membrane lesions associated with pulmonary inflammation and damage in the acute phase and gradually declined until recovery at the end time point. The severity of the lesions

correlated with the increasing concentration of total protein in BALF. These results suggest that UFCSs exposure induced pulmonary basement membrane destruction, leading to alterations in the permeability of the alveolar-capillary barrier resulted in the leakage of the transudation of serum proteins from the vasculature into alveolar lumens.

Johnston et al. (2000) reported that inhalation exposure to high dose of amorphous silica induced fragmented DNA damage of bronchiolar epithelial cells and alveolar macrophages that will be either repaired or results in cell death through apoptosis or necrosis. In the present study, many TUNEL positive cells were observed in lungs of UFCSs-treated mice compared to those of the control groups. Apoptotic cells were determined with careful observation of TUNEL-stained sections and serial H&E-stained sections because some necrotic cells could be also TUNEL-positive. If TUNEL-positive cells did represent histological features of necrosis in H&E-stained sections, they were not considered to be apoptotic cells. The TUNEL-positive stains were found in bronchiolar epithelium, lung parenchymal cells and active AMs. There was a significant and considerable increase of the apoptotic index, as assessed by TUNEL assay, in the lung parenchyma at all observation time points but transient increase in bronchial epithelial cells after instillation with 30 μg UFCSs. These results suggest that even a small dose (30 μg) of UFCSs can cause apoptosis of lung parenchymal cells.

Ultrafine particles have been reported to cause oxidative stress as a result of generation of reactive oxygen species in a number of in vivo and in vitro studies (Brown et al., 2001; Dick et al., 2003; Donaldson and Stone, 2003). 8-hydroxydeoxyguanosine (8-OHdG) is one of the most specific and representative of base modification among oxidative DNA damage products (Kasai, 1997). Hydroxyl radical, singlet oxygen, and peroxynitrite

are proposed to produce 8-OHdG (Warita et al., 2001). There is evidence to suggest that 8-OHdG is a major mutagenic lesion, producing predominately G→T transversion mutations (Kuchino et al., 1987). Immunohistochemical detection of 8-OHdG was recently established as a useful marker indicative of oxidative stress in various paraffin-embedded tissues (Gottschling et al., 2001; Takahashi et al., 1998). In this study, positive stains for 8-OHdG antibody were observed mainly in the cytoplasm and partially in the nuclei of bronchiolar epithelial cells, alveolar epithelial cells and activated AMs. The progression of immunopositivity of 8-OHdG was correlated to pulmonary lesions induced by exposure to UFCSs. These results suggest that oxidative damage may play an important role in the development of pulmonary inflammation and injury after instillation of UFCSs. The mechanism of the generation of the oxidative stress is not understood, but appears to be related to the large surface area of particles. Silicon functionalities as well as traces of iron impurities on the silica surface are implicated in free radical release at the surface and in subsurface layers of particles (Vallyathan et al., 1988; Fubini et al., 1990). Furthermore, a specific binding of silanol groups (SiOH) of silica to the phosphate groups of DNA was reported (Mao et al., 1994). This close proximity between DNA and the active sites of the silica surface would enable the short-lived radicals to induce DNA damage (Saffiotti et al., 1994). Free radicals from the particle surface can cause transcripts of pro-inflammatory gene products via oxidative stress responsive transcript factors (Donaldson et al., 1996). This could lead to the inflammatory response. Moreover, reactive oxygen species may be generated during phagocytosis of particles, leading to enhancement of oxidative stress.

In summary, this study demonstrated the pulmonary biological and pathological responses after intratracheal instillation of low dose of UFCSs in mice during the acute and

subacute stages. Low dose of UFCSs produced moderate inflammation and tissue damage on the lungs of mice during the acute period, but these responses were not sustained through a 30-day period after instillation and almost recovery at the subacute stage. Furthermore, our current study found that UFCSs can induce oxidative damage and apoptosis, which may be underlying causes of the lung tissue injury. The data from the dose and time responses in this study may be useful in predicting the acute and subacute effects of UFCSs on lungs.

Figures and figure legends

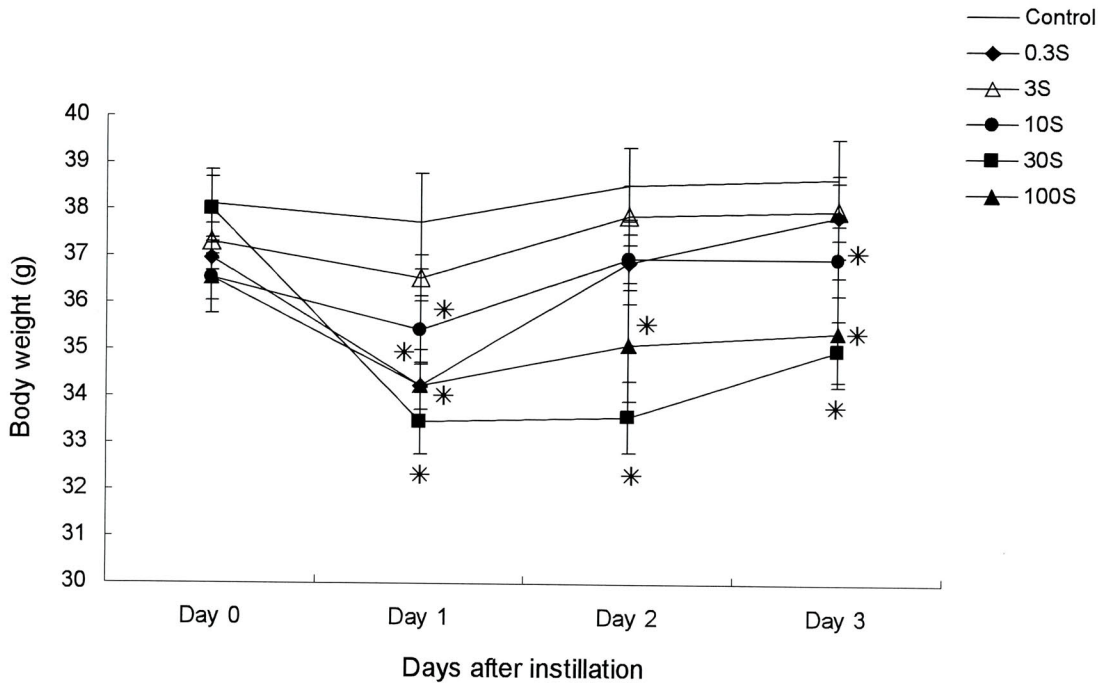

Figure 1. Body weight of mice after 1 to 3 days after instillation of various doses of UFCSs. Each data point represents the mean of 4 animals. Statistically significant differences from controls ($p < 0.05$).

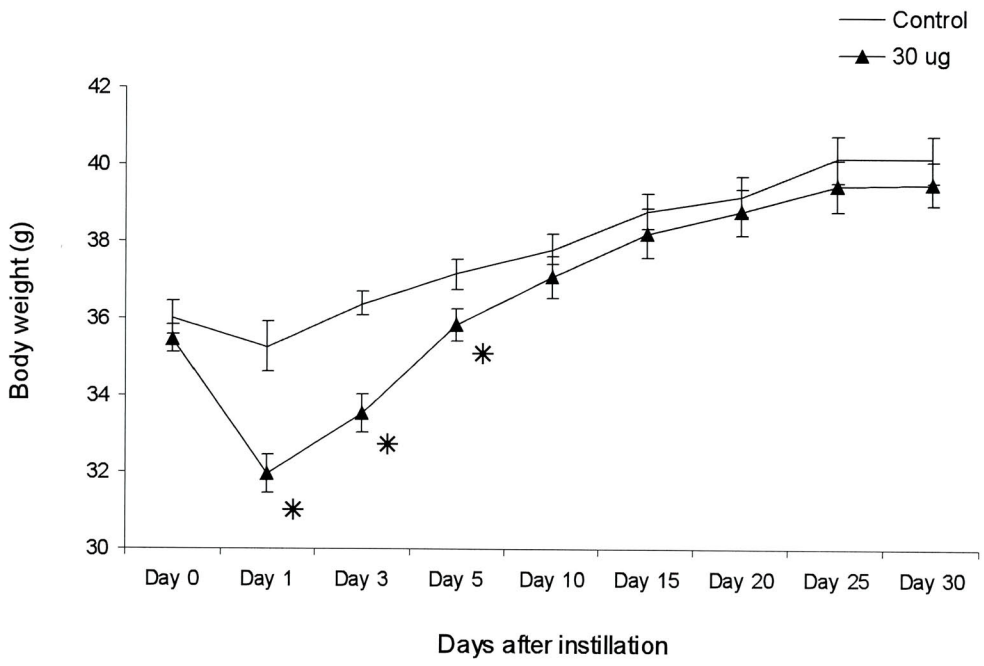

Figure 2. Body weight of mice after 1 to 30 days after instillation of 30 μg of UFCSs. Each data point represents the mean of 7- 9 animals. Statistically significant differences from controls ($p < 0.05$).

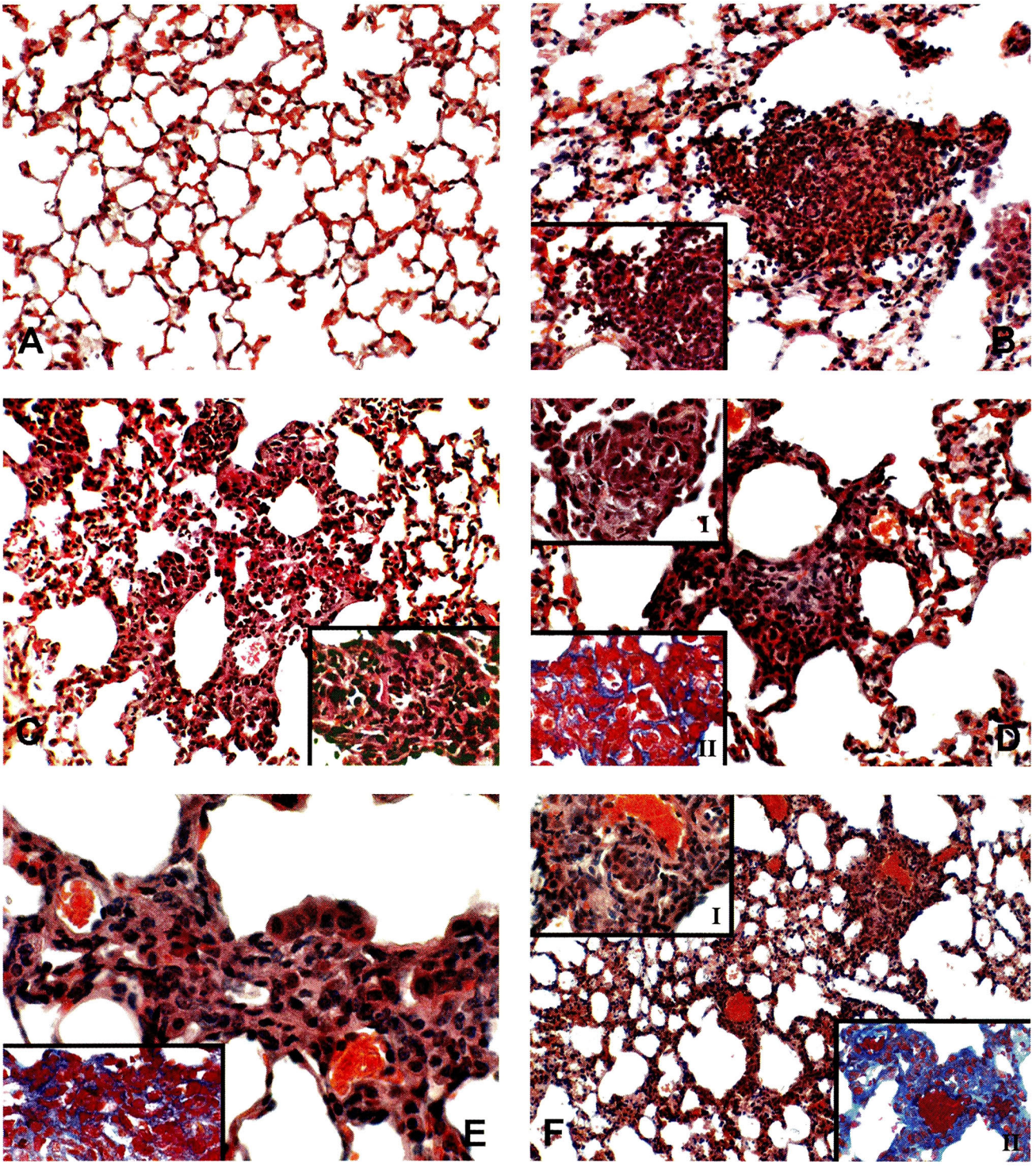
A
B
C
I
II
D
E
I
F
II

Figure 3. Photomicrographs from the lungs of control and UFCSs-treated mice sacrificed at various time points. H&E stain. (A) No inflammatory changes were observed in the lungs from the control groups. 190×. (B) UFCSs-treated mice sacrificed at 1 day after exposure showed moderate infiltration of neutrophils with an inflammatory nodule in alveolar air spaces. 190×. *Inset:* Higher magnification of inflammatory infiltration. 750×. (C) Mice sacrificed at 3 days after instillation with UFCSs showed moderate focal alveolitis especially in alveolar duct. 190×. *Inset:* the inflammatory focus consisting of particle-laden alveolar macrophages, neutrophils and fewer lymphocytes. 650×. (D) Foci of aggregation of particle-laden alveolar macrophages, lymphocytes and fewer fibroblasts were seen in UFCSs-treated mice sacrificed at 7 days after exposure. 190×. Higher magnification (inset I; 600×) and Azan stain (inset II; 600×) of the aggregated focus. (E) At 15 days after exposure, the occasional inflammatory foci characterized by accumulation of particle-laden alveolar macrophages, lymphocytes and fibroblasts were noted in lungs of UFCSs-treated mice. 450×. *Inset:* Azan stain of the inflammatory foci with fibrosis. 700×. (F) Thickening of alveolar walls associated with some areas of interstitial fibrosis was seen in lung tissues from UFCSs-treated mice sacrificed at 30 days post-exposure. 150×. *Inset I:* higher magnification of alveolar wall thickening. 600×. *Inset II:* Azan stain of the interstitial fibrosis in a perivascular area. 500×.

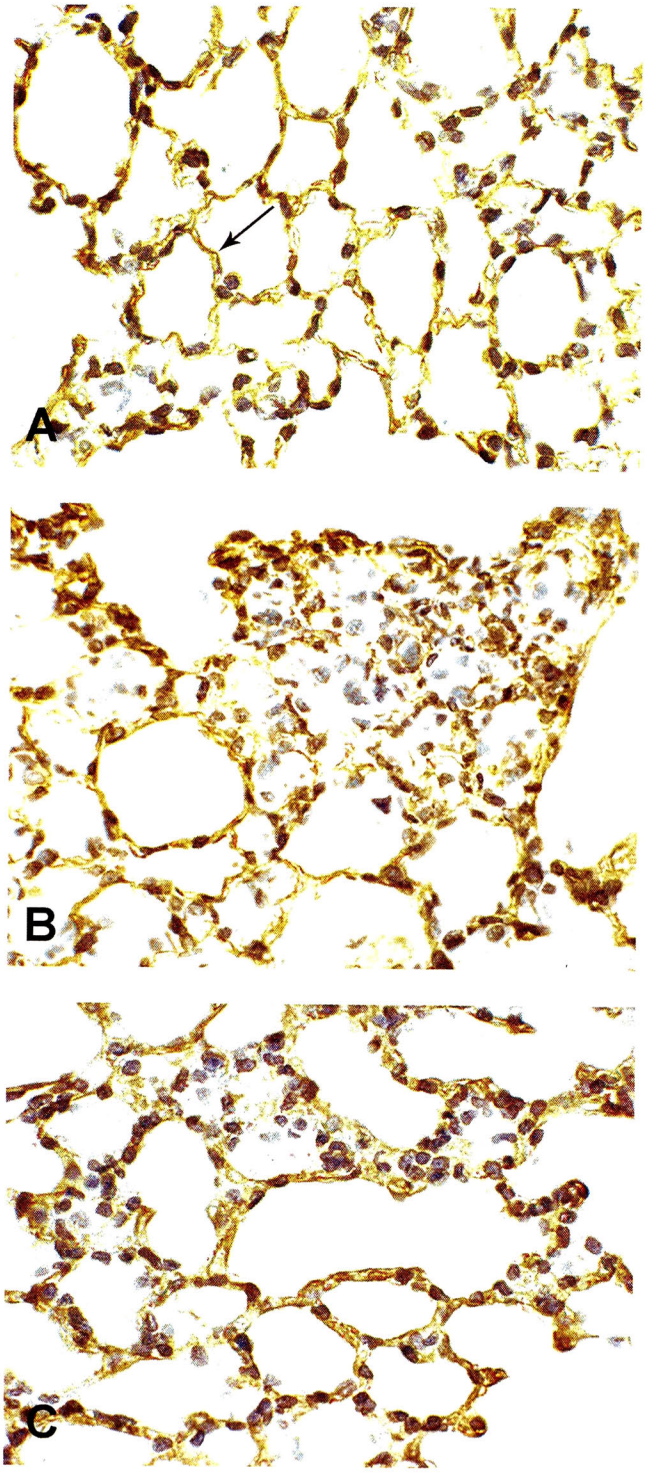
A
B
C

Figure 4. Laminin immunohistochemistry in lungs of control and UFCSs-treated mice sacrificed up to 30 days post-exposure. (A) Brown thin string-like positive staining was predominantly localized along alveolar basement membranes (arrow) in control animals. (B) UFCSs-treated mice sacrificed at 3 days post-exposure show weakly positive discontinuities in the basement membranes of alveoli especially in the site of focal alveolitis. (C) At 30 days after instillation, lungs from UFCSs-treated mice showed mainly positive patterns similar to the control groups; weak and discontinuous positive patterns of alveolar basement membrane were, however, seen in some areas of alveolar wall thickening. All illustrations are of the same magnification. 450×.

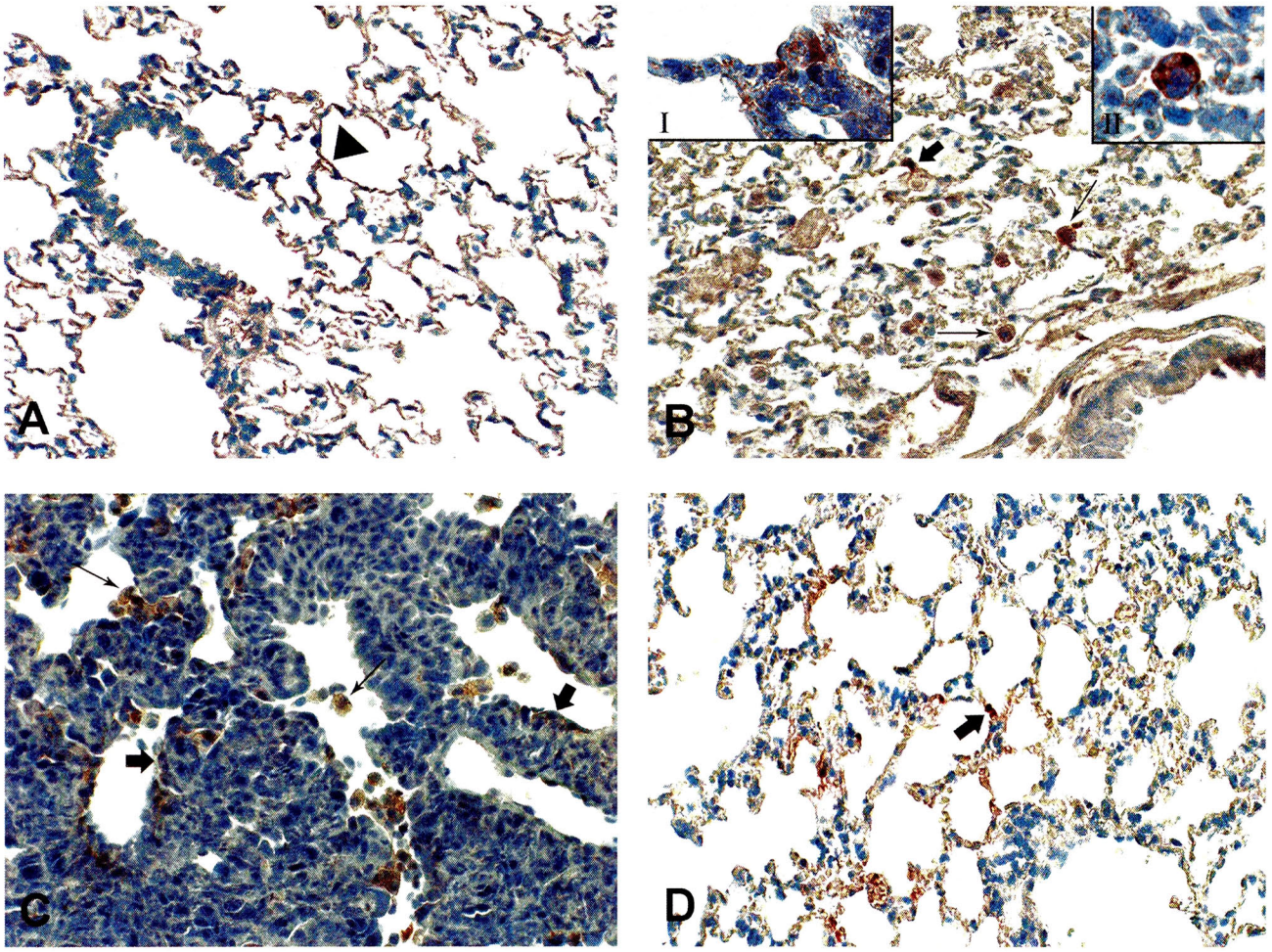
A
B
I
II
C
D

Figure 5. Immunohistochemical localization of 8-OHdG in lungs of control and UFCSs-treated mice killed at various time points. (A) Faint red positive staining was observed in alveoli in control animals (arrowhead). 190×. (B) In UFCSs-treated mice killed at 1 day post-exposure, intense red immunostaining appeared in a large number of macrophages (arrows) and some alveolar epithelial cells (solid arrow). 190×. The positive labeling was expressed mainly in the cytoplasm and occasionally in the nuclei of alveolar epithelial cell (inset I; 700×) and macrophage (inset II; 700×). (C) Positive immunostainings were observed in macrophages (arrows) around the sites of the aggregated foci of alveolitis and some alveolar epithelial cells (solid arrows) in lungs of UFCSs-treated mice killed at 3 days post-exposure. 190×. (D) In UFCSs-treated mice after 15 days, some alveolar epithelial cells showed positive staining in their cytoplasm (solid arrow). 190×.

GENERAL CONCLUSIONS

In the first chapter, the study aimed to contribute to the understanding of acute inflammatory events in the lung following colloidal silica exposure. An intratracheal instillation study to high doses of UFCSs and FCSs in mice was designed and carried out for examined pulmonary changes using pathological evaluations. At the early observation times, there was the evidence of severe degeneration and necrosis of bronchiolar epithelial cells with clumps of colloidal silica particles on epithelial cell surface, but no evidence of inflammatory reactions around the affected bronchioles. This suggested that colloidal silica particles might have a direct toxic effect on lung epithelial cells. The composition and structure of silica particle surface functionalities such as hydrophilicity, iron impurities and specific surface silanol groups (SiOH) may play an important role in these biological responses. Another specific objective of chapter 1 was to compare acute pathological findings of lung between UFCSs and FCSs treated animals. To our knowledge, there is no detailed pathological report on the pulmonary toxicity induced by different particle sizes of colloidal silica. The results showed that instillation of UFCSs induced more severe bronchiolar epithelial cell necrosis and purulent inflammation in alveoli than FCSs at 12 and 24 hr post-exposure. Laminin immunopositivity in UFCSs treated animals was weaker than those in the FCSs treated animals. These basement membrane damages were associated with particle accumulation. Concomitant ultrastructural studies confirmed more severe damage including dissociation of basement membranes and erosion of type I alveolar epithelial cell in UFCSs treated animals than FCSs treated animals. The higher toxicity of ultrafine particles than fine particles may be related to their larger surface area

and higher numbers per given mass. Higher surface area of particles can play a role as a carrier for co-pollutants or specifically transition metals, and a generator of reactive oxygen species on their surfaces. High numbers of ultrafine particles in the alveolar region may overwhelm the capacity of alveolar macrophages to phagocytoze and allow interaction of particles with epithelial cells, resulting in decreased clearing efficiency of ultrafine particles from the alveoli and leading to epithelial cell injury. In summary, the study in the first chapter showed the detailed pathology of severe acute pulmonary inflammation and tissue injury induced by intratracheal instillation of high dose of colloidal silica; ultrafine colloidal silica particles induced more severe changes than fine colloidal silica particles. Larger surface area of particles might be an important factor in the induction of lung tissue injury.

In chapter 2, the aim of this study was to determine the biological and pathological effects of intratracheally instilled low dose of UFCSs on the lungs of mice in terms of dose and time response during the acute and subacute stages. To study dose response, we exposed mice to different doses of UFCSs. The results showed that instillation of 30 or 100 μg UFCSs produced moderate to severe pulmonary inflammation and tissue injury. To investigate time effect, mice were instilled with 30 μg of UFCSs and sacrificed at intervals from 1 to 30 days after instillation. UFCSs induced moderate pulmonary inflammation and injury on BALF indices, concomitant histopathological and laminin immunohistochemical findings at an early stage, but this effect gradually decreased during the experiment. TUNEL analyses in UFCSs-treated animals showed a significant increase of the apoptotic index in lung parenchyma at all observation times. 8-OHdG immunolabellings were observed in bronchiolar epithelial cells, alveolar epithelial cells and activated AMs, which

correlated to pulmonary lesions induced by exposure to UFCSs. In summary, the study in the second chapter demonstrated that instillation of low dose of UFCSs can cause transient acute moderate lung inflammation and tissue damage. The induction factors of pulmonary toxicity of UFCSs may be oxidative stress and apoptosis.

Ultrafine colloidal silica particles are currently interest for a variety of applications in electronics, paints, ceramics, glass fiber, batteries, health care and industrial polishing. The market for this material is estimated to grow rapidly world wide. In the near future, UFCSs might be used in general consumer products, which are used by millions. However, there are limited data of evaluating safety levels and an understanding of the impact of this UFCSs on the environment, biological species and human health (either occupational or non-occupational exposure). In this study, it is important to note that the findings presented in this thesis apply to laboratory animal exposure to ultrafine colloidal silica during acute and subacute phases only. However, in order to gain a more complete understanding of toxicology and potential exposure levels of UFCS. Subchronic toxicity studies should be carry out not only in laboratory animals but also in humans (especially in high risk workers).

The animals in the present study were exposed via a bolus exposure technique, intratracheal instillation, which provides widespread delivery of actual small doses of particles throughout the lung but delivers those particles at a single time point. To simulate expected human exposure, compare particle deposition and pulmonary responses, the traditional inhalation toxicology study should be evaluated at various exposure and observation times.

The no-observable-effect level (NOEL) of colloidal silica (Ludox®) from previous traditional inhalation toxicity studies was determined to be 10 mg/m^3 or 489 μg/lung (Lee and Kelly, 1992; Warheit et al., 1991).. From the results of dose responses in chapter 2, pulmonary effects were still observed in mice exposed to 0.3, 3 or 10 μg UFCSs. Theses imply that the NOEL of our UFCSs might be less than 0.3 μg/lung. These data may be useful in predicting the acute and subacute effects of UFCSs on lungs and used as quantitative references to estimate exposure limit for occupational exposure.

ACKNOWLEDGMENTS

The research for this PhD-thesis was carried out at Department of Veterinary Pathology, Faculty of Agriculture, Tottori University. My sincere appreciation and gratitude belong to my principal supervisor Professor Dr. Akinori Shimada (Tottori University) for his firm guidance and pragmatic touch throughout this work. I am deeply grateful to my co-supervisor Associate Professor Dr. Takehito Morita (Tottori University) for sharing his amazing scientific insight, and for his dedication and encouragement during this work. I also wish to thank my co-supervisor Professor Dr. Toshiharu Hayashi (Yamaguchi University) for his expert advice and encouragement during the whole course of this thesis work. Additional thanks belong to Assistant Professor Dr. Masumi Sawada (currently in National Institute for Minamata Disease, Japan) for what she has taught me and her assistance in this work. I also want to thank all the other co-authors for their contributions in this work.

I would like to thank Ms. Eiko Kawahara for her excellent assistance in electron microscopy at Tottori University.

I warmly thank my collaborators in the nanoparticle research group, Miss Natsuko Kawamura, Miss Mina Okajima and Miss Hiromi Inoue for their fruitful collaboration. I am grateful to the whole students of Department of Veterinary Pathology, Tottori University for their continuous support and assistance.

My sincere appreciation and gratitude belong to all of my colleagues and staffs in Pathology Unit, Department of Veterinary Pathology, Chulalongkorn University (Thailand) for the unconditional support I received from them.

I wish to express my heartfelt gratitude to all my friends either in Japan or in Thailand for their relaxing company and for giving me chances to take my mind off the work.

Finally, I am especially grateful to my family for their never-ending love, the encouragement given to me, and for supporting me in all my efforts by over the years.

REFERENCES

American Thoracic Society. (1997). Adverse effects of crystalline silica exposure (ATS statement). *Am. J. Respir. Crit. Care Med.* **155**, 761-765.

Aumailley, M., and Smyte, N. (1998). The role of laminins in basement membrane function. *J. Anat.* **193,** 1-21.

Baggs, R.B., Ferin, J., and Oberdorster, G. (1997). Regression of pulmonary lesions produced by inhaled titanium dioxide in rats. *Vet. Pathol.* **34**, 592-597.

Brown, D.M., Stone, V., Findlay, P., MacNee, W., and Donaldson, K. (2000). Increased inflammation and intracellular calcium caused by ultrafine carbon black is independent of transition metals or other soluble components. *Occup. Environ.Med.* **57**, 685-691.

Brown, D.M., Wilson, M.R., MacNee, W., Stone, V., and Donaldson, K. (2001). Size-dependent proinflammatory effects of ultrafine polystylene particles: a role for surface area and oxidative stress in the enhanced activity of ultrafines. *Toxicol. Appl. Pharmacol.* **175**, 191-199.

Brunekreef, B., and Holgate, S.T. (2002). Air pollution and health. *Lancet* **360,** 1233-1242.

Callis, A.H., Sohnie, P.G., Mandel, G.S., Wiessner, J., and Madel, N.S. (1985). Kinetics of inflammatory and fibrotic pulmonary changes in a murine model of silicosis. *J. Lab. Clin. Med.* **105**, 547-553.

Choudat, D., Frisch, C., Barrat, G., el Kholti, A., and Conso, F. (1990). Occupational exposure to amorphous silica dust and pulmonary function. *Br. J. Ind. Med.* **47**, 763-6.

Costa, D.L., Lehmann, J.R., Winsett, D., Richards, J., Ledbetter, A.D., and Dreher, K.L. (2006). Comparative pulmonary toxicological assessment of oil combustion particles following inhalation or instillation exposure. *Toxicol. Sci.* **91**, 237-246.

Delfino, R.J., Sioutas, C., and Malik, S. (2005). Potential role of ultrafine particles in associations between airborne particle mass and cardiovascular health. *Environ. Health Perspect.* **113**, 934-946.

Dick, C.A.J., Brown, D.M., Donaldson, K., and Stone, V. (2003). The role of free radicals in the toxic and inflammatory effects of four different ultrafine particles types. *Inhal. Toxicol.* **15,** 39-52.

Donaldson, K., Beswick, P.H., and Gilmour, P.S. (1996). Free radical activity associated with the surface of particles: a unifying factor in determining biological activity. *Toxicol. Lett.* **88,** 293–298.

Donaldson, K., Gilmour, M.L., and Macnee, W. (2000). Asthma and PM_{10}. *Respir. Res.* **1**, 12-15.

Donaldson, K., and MacNee, W. (2001). Potential mechanisms of adverse pulmonary and cardiovascular effects of particulate air pollution (PM_{10}). *Int. J. Hyg. Environ. Health* **203,** 411-415.

Donaldson, K., and Stone, V. (2003). Current hypotheses on the mechanisms of toxicity of ultrafine particles. *Ann. Ist. Super. Sanita.* **39**, 405-410.

Donaldson, K., Stone, V., Clouter, A., Renwick, L., and MacNee, W. (2001). Ultrafine particles. *Occup. Environ. Med.* **58,** 211-216.

Dye, J.A., Lehman, J.R., McGee, J.K., Winsett, D.W., Ledbetter, A.D., Everitt, J.I., Ghio, A.J., and Costa, D.L. (2001). Acute pulmonary toxicity of particulate matter filter extracts in rats; coherence with epidemiologic studies in Utah Valley residents. *Environ. Health Perspect.* **109**, 395-403.

Frampton, M.W. (2001). Systemic and cardiovascular effects of airway injury and inflammation: ultrafine particle exposure in humans. *Environ. Health Perspect.* **109**, 529-532.

Fubini, B., Giamello, E., Volante, M., and Bolis, V. (1990). Chemical functionalities at the silica surface determining its reactivity when inhaled. Formation and reactivity of surface radicals. *Toxicol. Ind. Health* **6,** 571-98.

Fubini, B., Zanetti, G., Altilia, S., Tiozzo, R., Lison, D., and Saffiotti, U. (1999). Relationship between surface properties and cellular responses to crystalline silica: studies with heat-treated cristobalite. *Chem. Res. Toxicol.* **12**, 737-745.

Gil, J., and Hernadez, A.M. (1984). The connective tissue of the rat lung: electron immunohistochemical studies. *J. Hist. Cyt.* **32,** 230-238.

Gilmour, P.S., Brown, D.M., Beswick, P.H., Benton, E., Macnee, W., and Donaldson, K. (1997). Surface free radical activity of PM10 and ultrafine titanium dioxide: a unifying factor in their toxicity? *Ann. Occup. Hyg.* **41,** 32-38.

Gilmour, P.S., Ziesenis, A., Morrison, E.R., Vickers, M.A., Drost, E.M., Ford, I., Karg, E., Mossa, C., Schroeppel, A. Ferron, G.A., Heyder, J., Greaves, M., MacNee, W., and Donaldson, K. (2004). Pulmonary and systemic effects of short-term inhalation exposure to ultrafine carbon black particles. *Toxicol. Appl. Pharmacol.* **195**, 35-44.

Gottschling, B.C., Maronpot, R.R., Hailey, J.R., Peddada, S., Moomaw, C.R., Klaunig, J.E., and Nyska, A. (2001). The role of oxidative stress in indium phosphide-induced lung carcinogenesis in rats. *Toxicol. Sci.* **64,** 28–40.

Hagler Bailly Services, Inc. Health Effects of Particulate Matter Air Pollution in Bangkok (Executive Summary). (1998). A report prepared for Pollution Control Department, Ministry of Science, Technology and Environment, Bangkok, Thailand.

Hemenway, D.R., Absher, M.P., Fubini, B., and Bolis, V. (1993). What is the relationship between hemolytic potential and fibrogenicity of mineral dusts? *Arch. Environ. Health* **48**, 343-347.

Jaques, P.A., and Kim, C.S. (2000). Measurement of total lung deposition of inhaled ultrafine particles in healthy men and women. *Inhal. Tox.* **12,** 715-731.

Johnston, C.J., Driscoll, K.E., Finkelstein, J.N., Baggs, R., O'Reilly, M.A., Carter, J., Gelein, R., and Oberdorster, G. (2000). Pulmonary chemokine and mutagenic responses in rats after subchronic inhalation of amorphous and crystalline silica. *Toxicol. Sci.* **56,** 405-413.

Kaewamatawong, T., Kawamura, N., Okajima, M., Sawada, M., Morita, T., and Shimada, A. (2005). Acute pulmonary toxicity caused by exposure to colloidal silica: particle size dependent pathological changes in mice. *Tox. Pathol.* **3,** 745-751.

Kasai, H. (1997). Analysis of a form of oxidative DNA damage, 8-hydroxy-2X-deoxyguanosine, as a marker of cellular oxidative stress during carcinogenesis. *Muta. Res.* **387,** 147–163.

Kelly, D.P., and Lee, K.P.(1990). Pulmonary response to Ludox colloidal silica inhalation exposure in rats. *Toxicologist* **10**, 202A.

Kuchino, Y., Mori, F., Kasi, H., Inoue, H., Iwai, S., Miura, K. M., Ohtsuka, E., and Nichimura, S. (1987). Misreading of DNA templates containing 8-hydroxydeoxyguanosine at the modified base and at adjacent residues. *Nature (Lond.)* **327,** 77-79.

Kreyling, W.G., Semmler-Behnke, M., and Moller, W. (2006). Ultrafine particle-lung interactions: does size matter? *J. Aerosol. Med.* **19**, 74-83.

Lee, K.P, and Kelly, D.P. (1992). The pulmonary response and clearance of Ludox colloidal silica after a 4-week inhalation exposure in rats. *Fundam. Appl. Toxicol.* **19**, 399-410.

Lee, K.P., and Kelly, D.P. (1993). Translocation of particle-laden alveolar macrophages and intra-alveolar granuloma formation in rats exposed to Ludox colloidal amorphous silica by inhalation. *Toxicology* **77**, 205- 222.

Li, X.Y., Brown, D., Smith, S., Macnee, W., and Donaldson, K. (1999). Short-term inflammatory responses following intratracheal instillation of fine and ultrafine carbon black in rats. *Inhal. Toxicol.* **11**, 709-731.

Lugano, E.M., Dauber, J.H. and Daniele,R.P. (1982). Acute experimental silicosis. Lung morphology, histology, and macrophage chemotaxin secretion. *Am. J. Pathol.* **109**, 27-36.

Mao, Y., Daniel, L.N., Knapton A.D., Shi X., and Saffiotti, U. (1995). Protective effects of silanol group binding agents on quartz toxicity to rat lung alveolar cells. *Appl. Occup. Environ. Hygiene* **10**, 1132-1137.

Mao, Y., Daniel, L. N., Whittaker, N., and Saffiotti, U. (1994). DNA binding to crystalline silica characterized by Fourier-transform infrared spectroscopy. *Environ. Health Perspect.* **102**, 165-171.

McLaughlin, J.K., Chow, W.H., and Levy, L.S. (1997). Amorphous silica: a review of health effects from inhalation exposure with particular reference to cancer. *Toxicol. Environ. Health* **50**,553-66.

Merget, R., Bauer, T., Kupper, H.U., Philippou, S., Bauer, H.D., Breitstadt, R., and Bruening, T. (2002). Health hazards due to the inhalation of amorphous silica. *Arch. Toxicol.* **75**, 625-634.

Merriam Webster's Medical Desk Dictionary. (2002). Revised Edition. New York: Thomson Delmar Learning.

Nemmar, A., Hoet, P.H., and Vanquickenborne, B., Dinsdale, D., Thomeer, M., Hoylaerts, M.F., Vanbilloen, H., Mortelmans, L. and Nemery, B. (2002). Passage of inhaled particles into the blood circulation in humans. *Circulation* **105**, 411-414.

Nemmar, A., Hoylaerts, M. F., Hoet, P.H.M., Dinsdale, D., Smith, T., Xu, H., Vermylen, J., and Nemery, B. (2002). Ultrafine particles affect experimental thrombosis in an In vivo hamster model. *Am. J. Respir. Crit. Care Med.* **166**, 998–1004.

Nemmar, A., Hoylaerts, M. F., Hoet, P.H.M., Vermylen, J., and Nemery, B. (2003). Size effect of intratracheally instilled particles on pulmonary inflammation and vascular thrombosis. *Toxicol. App. Pharmacol.* **186**, 38–45.

Oberdorster, G. (2001). Pulmonary effects of inhaled ultrafine particles. *Int. Arch. Occup. Environ. Healt* **74,** 1-8.

Pandurangi, R.S., Seehra, M.S., Razzaboni, B.L., and Bolsaitis, P. (1990). Surface and bulk infrared modes of crystalline and amorphous silica particles: a study of the relation of surface structure to cytotoxicity of respirable silica. *Environ. Health Perspect.* **86**, 327-336.

Pope, C.A., Burnett, R.T., Thun, M.J., Calle, E.E., Krewski, D., Ito, K., and Thurston, G.D. (2002). Lung cancer, cardiopulmonary mortality, and long-term exposure to fine particulate air pollution. *J. Am. Med. Assoc.* **287**, 1132-1141.

Pope III, C. A., (2000). Epidemiology of fine particulate air pollution and human health: Biologic mechanisms and who's at risk? *Environ. Health Perspec.* **108**, 713-723.

Pratt, P.C. (1983). Lung dust content and response in guinea pigs inhaling three forms of Silica. *Arch. Eviron. Health* **38**, 197-204.

Public Health College, Chulalongkorn University. (1995). Survey of health effect of airborne dust to Bangkok resident and its trend. A report prepared for Bureau of Environmental Health, Ministry of Public Health, Bangkok, Thailand.

Reiser, K.M., Hesterberg, T.W., Haschek, W.M. and Last, J.A. (1982). Experimental silicosis. I. Acute effects of intratracheally instilled quartz on collagen metabolism and morphologic characteristics of rat lungs. *Am. J. Pathol.* **107**, 176-185.

Renwick, L. C., Donaldson, K., and Clouter, A. (2001). Impairment of alveolar macrophage phagocytosis by ultrafine particles. *Toxicol. Appl. Pharmacol.* **172**, 119–127.

Reuzel, P. G. J., Bruijntjes, J. P., Feron, V. J., and Woutersen, R. A. (1991) Subchronic inhalation toxicity of amorphous silicas and quartz dust in rats. Food. *Chem. Toxicol.* **29**, 341-354.

Saffiotti, U., Daniel, L. N., Mao, Y., Shi, X., Williams, A. O., and Kaighn, M.E. (1994). Mechanisms of carcinogenesis by crystalline silica in relation to oxygen radicals. *Environ. Health Perspect.* **102**, 159-163.

Samet, J.M., Dominici, F., Curriero, F.C., Coursac, I., Zeger, S.L. (2000). Fine particulate air pollution and mortality in 20 US Cities, 1987-1994. *N. Engl. J. Med.* **343**, 1742-1749.

Shi, X.L., Dalal, N.S., Hu, X.N., Vallyathan, V. (1989). The chemical properties of silica particle surface in relation to silica-cell interactions. *J. Toxicol. Environ. Health* **27**, 435-454.

Takahashi, S., Hirose, M., Tamano, S., Ozaki, M., Orita, S., Ito, T., Takeuchi, M., Ochi, H., Fukada, S., Kasai, H., and Shirai, T. (1998). Immunohistochemical detection of 8-hydroxy-2`-deoxyguanosine in paraffin-embedded sections of rat liver after carbon tetrachloride treatment. *Toxicol. Pathol.* **26,** 247–252.

United States Environmental Protection Agency (USEPA). (1996). Ambient levels and noncancer health effects of inhaled crystalline and amorphous silica: health issue assessment. Research Triangle Park, NC: Office of Research and Development; EPA report no. EPA/600/R-95/115.

United States Environmental Protection Agency (USEPA). (2004). Air quality criteria for particulate matter. Publication EPA/600/P-99/002aF. Research Triangle Park, NC: USEPA Office of Research and Development, National Center for Environmental Assessment – RTP Office.

Vallyathan, V., Shi, X. L., Dalal, N. S., Irr, W., and Castranova, V. (1988).Generation of free radicals from freshly fractured silica dust. Potential role in acute silica-induced lung injury. *Am. Rev. Respir. Dis.* **138**, 1213-1219.

Van Niekerk, W.C.A., Fourie, M.H., and Mouton, G. (2002). Investigation of crystalline phases in silica fume. SIMRAC project support services.SIM 020601.

Warheit, D.B. (2004). Nanoparticles: health impacts?. *Materialstoday* : the DuPont company, DE. **February**, 32-35.

Warheit, D.B., Carakostas, M.C., Kelly, D.P., and Hartsky, M.A. (1991). Four-week inhalation toxicity study with Ludox colloidal silica in rats: pulmonary cellular responses. *Fundam. Appl. Toxicol.* **16**, 590-601.

Warheit, D.B., McHugh, T.A., and Hartsky, M.A. (1995). Differential pulmonary responses in rats inhaling crystalline, colloidal or amorphous silica dusts. *Scand. J. Work Eviron. Health* **21**, 19-21.

Warita, H., Hayashi, T., Murakami, T., Manabe, Y., and Abe, K. (2001). Oxidative damage to mitochondrial DNA in spinal motoneurons of transgenic ALS mice. *Mol. Brain. Res.* **89,** 147–152.

Weijers, E. P., Khlystov, A. Y., Kos, G. P. A. and Erisman, J. W. (2004). Variability of particulate matter concentrations along roads and motorways determined by a moving measurement unit. *Atmos. Environ.* **38**, 2993-3002.

World Bank. (1996). *The World Urbanization Prospects*, DESA, New York.

World Health Organization (WHO). (2003). Health aspects of air pollution with particulate matter, ozone and nitrogen dioxide. Report EUR/03/5042688 of working group, Bonn, Germany, 13-15 January 2003. Copenhagen, Denmark: WHO Regional Office for Europe.

Zhang, Q., Kusaka, Y., and Donaldson, K. (2000). Comparative pulmonary responses caused by exposure to standard cobalt and ultrafine cobalt. *J. Occup. Health* **42**, 179-184.

Zhang, Q., Kusaka, Y., Sato, K., Mo, Y., Fukuda, M., and Donaldson, K. (1998a).Toxicity of ultrafine nickel particles in lungs after intratracheal instillation. *J. Occup. Health* **40**, 171–176.

Zhang, Q., Kusaka, Y., Sato, K., Nakakuki, K., Kohyama, N., and Donaldson, K. (1998b). Differences in the extent of inflammation caused by intratracheal exposure to three ultrafine metals: role of free radicals. *J. Toxicol. Environ. Health* **53**, 423-438.

Zhang, Q., Kusaka, Y., Zhu, X., Sato, K. Mo, Y., Kluz, T., and Donaldson, K. (2003). Comparative toxicity of standard nickel and ultrafine nickel in lung after intratracheal instillation. *J. Occup. Health* **45**, 23-30.